Report No. KSU-18-3 ▪ FINAL REPORT ▪ November 2024

Determining an Acceptable California Bearing Ratio (CBR) Value for Kansas Subgrades Based on Pavement Distress Data

Dunja Perić, Ph.D.
Gyuhyeong Goh, Ph.D.
Arash Saeidi Rashk Olia

Kansas State University Transportation Center

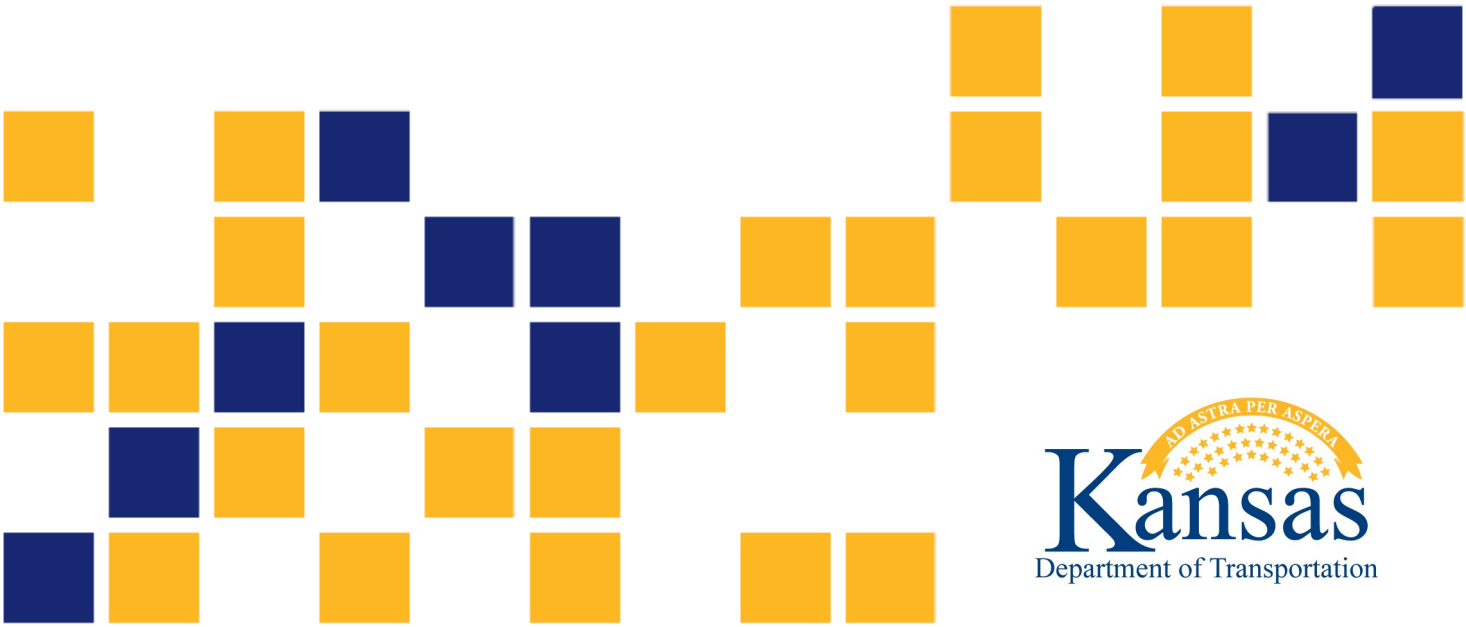

Kansas
Department of Transportation

1 Report No. K-TRAN: KSU-18-3	**2 Government Accession No.**	**3 Recipient Catalog No.**
4 Title and Subtitle Determining an Acceptable California Bearing Ratio (CBR) Value for Kansas Subgrades Based on Pavement Distress Data		**5 Report Date** November 2024 **6 Performing Organization Code**
7 Author(s) Dunja Perić, Ph.D.; Gyuhyeong Goh, Ph.D.; Arash Saeidi Rashk Olia		**8 Performing Organization Report No.**
9 Performing Organization Name and Address Kansas State University Transportation Center Department of Civil Engineering 2118 Fiedler Hall 1701C Platt Street Manhattan, KS 66506-5000		**10 Work Unit No. (TRAIS)** **11 Contract or Grant No.** C2121
12 Sponsoring Agency Name and Address Kansas Department of Transportation Bureau of Research 2300 SW Van Buren Topeka, Kansas 66611-1195		**13 Type of Report and Period Covered** Final Report April 2018 – December 2021 **14 Sponsoring Agency Code** RE-0728-01

15 Supplementary Notes
For more information write to address in block 9.

16 Abstract

The major objective of this study was to develop scientifically based recommendations for acceptable California Bearing Ratio (CBR) values for Kansas subgrades. To this end, multiple statistical analyses including: 1) Principal Component Regression Analysis (PCRA), 2) Regression Analysis (RA), 3) Multivariate Principal Component Regression Analysis (MPCRA), and 4) Multivariate Regression Analysis (MRA) were performed on in service flexible pavements in the state of Kansas. Statistically significant correlations were found between results of Dynamic Cone Penetrometer (DCP) tests conducted on subgrade soils and total rutting, fatigue cracking code one (FC1), percent of good pavement core, and percent of poor pavement core. Additional statistically significant correlations include the correlations between traffic volume and transverse cracking code one (TC1), and two (TC2), correlations between the thickness of unbound layer and pavement roughness, and percent of good core and percent of poor core. Corresponding equations are provided in the report.

Furthermore, x-y graphs depicting time in years needed for the unit increase in rutting severity code versus DCP or CBR value are provided. An additional set of graphs depicting percent of good core, poor core and fair core versus DCP or CBR value is also provided for different thicknesses of unbound layer. These graphs along with additional equations can be used to determine scientifically based acceptable values of CBR.

17 Key Words California Bearing Ratio (CBR), Dynamic Cone Penetrometer (DCP), pavement distress, statistical pavement performance prediction models, subgrade soil		**18 Distribution Statement** No restrictions. This document is available to the public through the National Technical Information Service www.ntis.gov.	
19 Security Classification (of this report) Unclassified	**20 Security Classification (of this page)** Unclassified	**21 No. of pages** 72	**22 Price**

This page intentionally left blank.

Determining an Acceptable California Bearing Ratio (CBR) Value for Kansas Subgrades Based on Pavement Distress Data

Final Report

Prepared by

Dunja Perić, Ph.D.
Gyuhyeong Goh, Ph.D.
Arash Saeidi Rashk Olia

Kansas State University Transportation Center

A Report on Research Sponsored by

THE KANSAS DEPARTMENT OF TRANSPORTATION
TOPEKA, KANSAS

and

KANSAS STATE UNIVERSITY TRANSPORTATION CENTER
MANHATTAN, KANSAS

November 2024

PREFACE

The Kansas Department of Transportation's (KDOT) Kansas Transportation Research and New-Developments (K-TRAN) Research Program funded this research project. It is an ongoing, cooperative, and comprehensive research program addressing transportation needs of the state of Kansas utilizing academic and research resources from KDOT, Kansas State University and the University of Kansas. Transportation professionals in KDOT and the universities jointly develop the projects included in the research program.

NOTICE

The authors and the state of Kansas do not endorse products or manufacturers. Trade and manufacturers names appear herein solely because they are considered essential to the object of this report.

This information is available in alternative accessible formats. To obtain an alternative format, contact the Office of Public Affairs, Kansas Department of Transportation, 700 SW Harrison, 2nd Floor – West Wing, Topeka, Kansas 66603-3745 or phone (785) 296-3585 (Voice) (TDD).

DISCLAIMER

The contents of this report reflect the views of the authors who are responsible for the facts and accuracy of the data presented herein. The contents do not necessarily reflect the views or the policies of the state of Kansas. This report does not constitute a standard, specification, or regulation.

Abstract

California Bearing Ratio (CBR) of subgrade soils, which can be used in design of flexible pavements, can be obtained from Dynamic Cone Penetrometer (DCP) tests through a statistical correlation. The main objective of this study was to determine an acceptable CBR value based on the use of statistical pavement performance evaluation models. To this end, actual DCP tests, along with the thickness of unbound layer and traffic data in the form of Average Annual Daily Truck Traffic (AADTT) were used as predictors for statistical analyses conducted in this study. Distress indicators of in-service pavements including total rutting, fatigue cracking, transverse cracking, roughness, and quality of pavement cores were the outcomes of the analyses.

All data were collected from 21 sections of largely flexible pavements of interstate and major highways across the state of Kansas. Only four pavement sections were composite pavements whereby the surface layer, which was made of asphalt concrete (AC), was underlain by a cement concrete layer. Four types of statistical analyses were performed including:

1. Principal Component Regression Analysis (PCRA),
2. Regression Analysis (RA),
3. Multivariate Principal Component Regression Analysis (MPCRA), and
4. Multivariate Regression Analysis (MRA).

Statistically significant correlations were found between:

- DCP and total rutting, DCP and fatigue cracking, DCP and percent of good core, and DCP and percent of poor core,
- AADTT and transverse cracking, and
- thickness of unbound layer and International Roughness Index (IRI), thickness of unbound layer and percent of good core, and thickness of unbound layer and percent of poor core.

Specifically, the results show that 54.73% of total rutting can be explained by DCP test results from depths of zero to 12.5 inches of subgrade soil, based on PCRA. In addition, 65.04% of total rutting can be explained by DCP test results conducted within the top 2.5 inches of subgrade soil, based on RA. Both correlations are significant at level 0.01. The correlations are

positive and linear, thus implying that as mean DCP values for a given pavement segment increase the corresponding total rutting tends to be higher. This leads to a negative correlation between the change in rutting severity code and CBR value. Based on the result of the RA analysis, x-y graphs that provide a number of years required for the unit increase in rutting severity code value versus DCP and/or CBR value have been constructed.

Additional statistically significant correlations that do not directly involve DCP test results are also discussed in the report.

Acknowledgments

The authors would like to thank the Kansas Department of Transportation for funding the research described in this report. The authors thank the KDOT project monitor Ryan Barrett (Bureau of Road Design), as well as Luke Metheny (Bureau of Structures and Geotechnical Services), and Nat Velasquez (Bureau of Road Design).

Table of Contents

List of Tables

List of Figures

Chapter 1: Introduction

Pavement is a composite structure that consists of several layers, which are made from different materials, including a surface layer, base layer, and subgrade layer. The performance of pavement depends on the behaviors of all these layers. Notwithstanding, Schwartz et al. (2013) showed that the performance predicted by the American Association of State Highways and Transportation Officials (AASHTO) AASHTOWare Pavement Mechanistic-Empirical ME Design shows low or no sensitivity to inputs from unbound and subgrade layers. Specifically, they found that total rutting in flexible pavements was only marginally sensitive to the resilient modulus of subgrade layers and non-sensitive to the thickness of unbound layers.

Total rutting is a pavement surface depression in a wheel path that is a consequence of a permanent deformation accumulated within all pavement layers. Rutting affects both the riding quality and structural health of flexible pavements. Consequently, it is considered to be a major failure mode of flexible pavements. Waseem and Yuan (2013) performed a local calibration of Mechanistic Empirical Pavement Design Guide (MEPDG) rutting models for flexible pavements and proposed percentage contributions from different pavement layers to the total rutting. Orobio and Zaniewski (2011) found that the resilient modulus of subgrade has the largest effect on rutting predicted from MEPDG. Baus and Stires (2010) suggested that the resilient modulus of subgrade layers had a significant effect on pavement roughness, total rutting, alligator cracking, and longitudinal cracking for a number of pavements in South Carolina. Thus, subgrade soil appears to have significant effects on the accumulation of different types of distress in flexible pavements.

Puppala, Saride, and Chomtid, (2009) found that resilient modulus did not fully account for rutting or permanent deformation of the subgrade layer. This is a reasonable finding because resilient modulus is an elastic property that is directly linked to recoverable deformation while rutting occurs due to a plastic or irrecoverable deformation. A direct subgrade layer strength parameter is not included in the MEPDG rut prediction model (AASHTO, 2008).

In this study subgrade properties are reflected within the results of Dynamic Cone Penetrometer (DCP) tests that were conducted on the top 12.5 inches of subgrade soils. The DCP test results can be converted to the corresponding California Bearing Ratio (CBR) values by

employing a statistical correlation. Furthermore, pavement distresses are linked to DCP test results, Average Annual Daily Truck Traffic (AADTT), and thickness of unbound layer through multiple statistical models that address performance of the selected in-service flexible pavements in the state of Kansas. The goal of statistical analyses is to identify the types of flexible pavement distresses that are correlated with DCP test results and to the CBR values of subgrade soils. The primary objective of this study is to determine scientifically acceptable CBR values for Kansas subgrades based on the predictions of pavement performance evaluation models. The secondary objective is to identify remaining statistically significant correlations resulting from the analyses.

Chapter 2: Literature Review

The major motivation for this study was discussed in the introduction. The methodology adopted to accomplish the stated goals was the use of statistical analyses. Hence, this chapter is focused primarily on the prior use of statistical models for the development of pavement performance prediction models.

Pavement performance prediction is extremely helpful for rational allocation of resources at the network level (Meegoda & Gao, 2014), and it can contribute towards increased money savings (Madanat, 1993). Future performance of pavements can be predicted based on known present and/or past pavement conditions along with the data representing the variables that control pavement deterioration.

Pavement performance evaluation models have been developed by several states in the USA and worldwide. Johnson and Cation (1992) developed a pavement performance model for North Dakota Department of Transportation (NDDOT) by using roughness index, distress index, and structural index. Chan, Oppermann, and Wu (1997) developed a pavement performance model for North Carolina Department of Transportation (NCDOT) based on the pavement condition rating. DeLisle, Sullo, and Grivas (2003) developed a network-level performance model based on the 20 years of historical data for pavements in the state of New York. Prozzi and Madanat (2004) developed pavement performance models for pavements in Minnesota by using regression techniques. S.-H. Kim and N. Kim (2006) found linear regression models to be effective predictors of pavement performance, while Mills, Attoh-Okine, and McNeil (2012) used simple and multiple regression models to predict pavement performance in Delaware.

International pavement performance studies were conducted by Henning, Costello, Dunn, Parkman, and Hart (2004) and Isa, Ma'soem, and Hwa (2005). Henning et al. (2004) used data from Long-Term Pavement Performance (LTPP) sites to calibrate pavement performance models in New Zealand. Isa et al. (2005) used regression techniques to develop pavement performance models for federal roads in Malaysia.

These pavement performance studies have demonstrated that statistical approach is a viable technique. Consequently, the statistical analyses are adopted in this study as a methodology for predicting performance of flexible pavements in Kansas. This approach facilitates development of scientifically based recommendations for acceptable CBR values of Kansas subgrade soils.

Chapter 3: Statistical Analyses

3.1 Introduction

This study is focused on the effects of primarily subgrade and secondarily unbound layer on performance of flexible pavements with the goal of determining a scientifically acceptable value of CBR. Luo, Gu, Zhang, Lytton, and Zollinger (2017) studied mechanistic-empirical models for better consideration of influence of subgrade and unbound layers on pavement performance. They pointed out that the factors that affect the pavement performance are material properties, material behaviors through which the materials respond to traffic and environmental conditions, and structural conditions such as the thickness of unbound layers. Consequently, the predictors selected for the statistical analyses that have been conducted, herein, are:

1. DCP tests on subgrade soils conducted in depths ranging from zero to 12.5 inches,
2. traffic volume data in the form of AADTT, and
3. the thickness of unbound layer.

Selected indicators of pavement performance are:

- total rutting,
- fatigue cracking,
- transverse cracking,
- pavement roughness, and
- quality of pavement cores.

3.2 Selected Pavement Segments

Pavement condition in Kansas is assessed based on pavement roughness and surface distress data that are collected by KDOT. Baus and Stires (2010) recommended that a minimum of 20 pavement segments should be used for calibrating and validating pavement distress conditions. To this end, 21 pavement segments were selected by KDOT in this study. Table 3.1 provides locations of the selected flexible pavement segments; whereby, EB and WB denote eastbound and westbound lanes, respectively. NB and SB denote northbound and southbound lanes. Additional information presented in Table 3.1 includes thicknesses of unbound layers, year

in which DCP tests were performed, and the year in which the last pavement treatments prior to DCP testing were applied. Figure 3.1 shows the location of the counties listed in Table 3.1, thus indicating that pavement segments were selected from geographically diverse regions of Kansas.

Table 3.1: Selected Flexible Pavement Segments

County	Location	Thickness of unbound layer (in.)	DCP year	Year of last treatment
Cherokee	US 166, EB & WB	6	2017	2016
Clay	US 24, EB & WB	0	2015	2011
Douglas	KS 10, EB & WB	0	2016	2013
Ford	US 50, EB & WB	0	2017	2012
Gove	I 70, EB & WB	0	2017	2009
Harper	US 160, EB & WB	0	2017	2007
Johnson3	I 435, NB & SB	0	2016	2013
Reno	KS 14, EB & WB	0	2017	2012
Shawnee1	US 24, EB & WB	0	2014	2012
Shawnee2	US 24, WB	4	2014	2012
Thomas	I 70, EB & WB	0	2017	2011

Historic pavement performance data were collected over relatively long time periods, throughout which several pavement treatments were applied. As shown in Table 3.1, DCP tests for the selected pavement sections were performed in years ranging from 2014 to 2017. The last treatments preceding DCP testing were applied in years ranging from 2007 to 2016. On average, the time difference between the application of the last treatment and year of DCP is 4.36 years. Therefore, the assumption that the average value of pavement distress indicators since the year of the last treatment tests can be correlated to DCP values is reasonable.

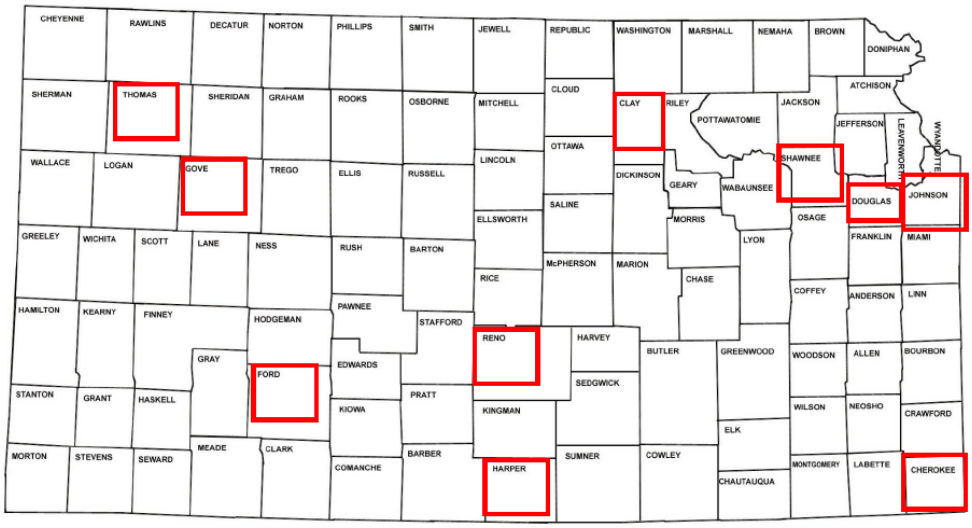

Figure 3.1: Location of Counties where Flexible Pavement Sections were Selected for Statistical Analyses

3.3 Pavement Distress Indicators

Beginning in 2013, all flexible pavement condition data were collected using an automated system that collects pavement intensity and range images. From 1982 until 1992, pavement roughness was determined by using a Mays meter. From 1993 until 1995, a South Dakota Profilometer equipped with sonic sensors was used. In 1995, South Dakota Profilometer sensors were converted from sonic to laser devices. The pavement distress indicators used in this study include:

- total rutting,
- fatigue cracking,
- transverse cracking,
- roughness, and
- core analysis.

Rutting is a longitudinal surface depression in the wheel path. Total rutting is a consequence of permanent deformation in each pavement layer. It is expressed in terms of rutting severity codes zero (0), one (1), two (2), and three (3) that correspond to rut depths of zero inches to 0.24 inches, 0.25 inches to 0.5 inches, 0.51 inches to 1 inch, and larger than 1 inch, respectively. While the rut depth of less than 0.5 inches is considered less severe (Shahin, 2005), rutting codes

two and three are flagged as “Rutting” and “RUTTING,” respectively. Figure 3.2 depicts the evolution of rutting severity code over time for Clay County. The corresponding average rate of change in rutting severity code since the last treatment is 0.333/year.

Fatigue cracking is expressed in lineal feet of fatigue cracking in a 100 ft sample. It is expressed in terms of codes one (FC1), two (FC2), three (FC3), and four (FC4). Code one describes hairline alligator cracking; whereby, the pieces are not removable. Code two corresponds to alligator cracking with spalled cracks and non-removable pieces. Code three describes alligator cracking with loose and removable pieces while pavement might pump. Code four describes the pavement that has shoved, thus forming a ridge of material adjacent to the wheel path. These definitions of different fatigue cracking codes come from KDOT Pavement Management Information Systems (PMIS). Figure 3.3 shows the evolution of FC1 versus time for Clay County. The corresponding average rate of change of FC1 since the last treatment is 1.333 ft/100ft/year.

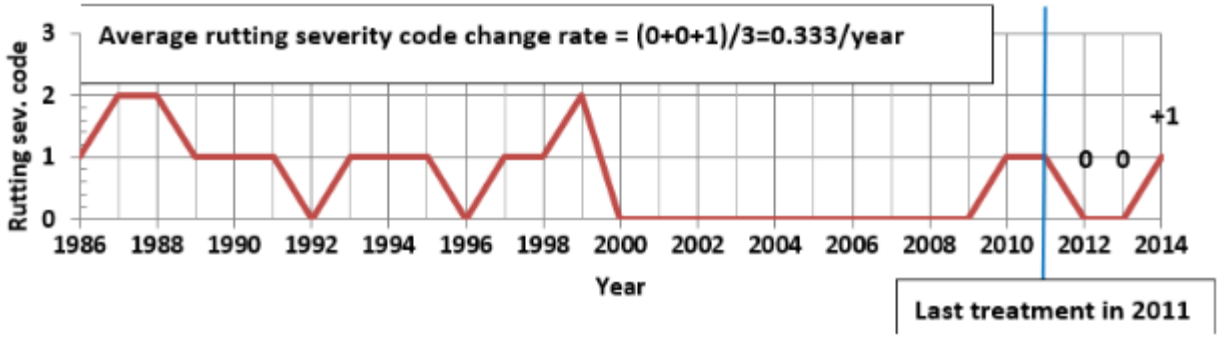

Figure 3.2: Rutting Severity Code versus Time for Clay County

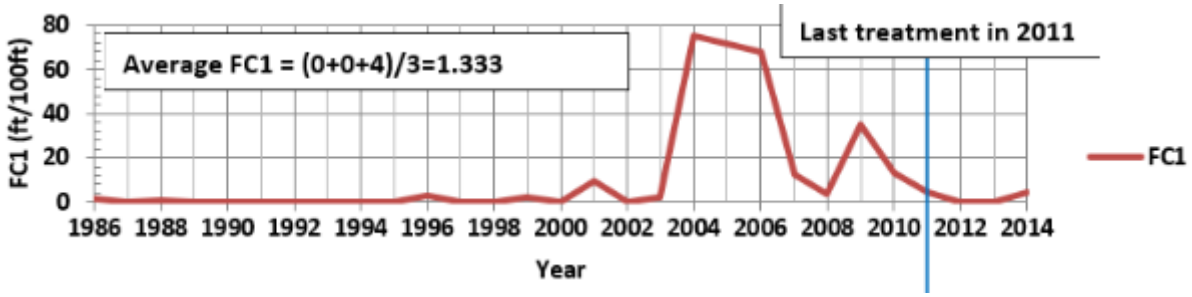

Figure 3.3: Fatigue Cracking Code One (FC1) versus Time for Clay County

Transverse cracking is expressed as a number of transverse cracks per 100 ft long pavement segment. It is expressed in terms of codes zero (TC0), one (TC1), two (TC2), and three (TC3). Code zero describes sealed transverse cracks with no roughness. Code one corresponds to 0.25 in. or wider cracks with no roughness and secondary cracking of less than 4 ft per lane or any width with failed seal (1 or more feet per lane). Code two describes cracks of any width with noticeable roughness due to a depression of bump. This includes cracks with more than 4 ft of secondary cracking without roughness. Code three describes cracks of any width with significant roughness due to depression of bump and with secondary cracking that is more severe than in case of code two. Figure 3.4 shows evolution of TC1, TC2 and TC3 versus time. The corresponding average rate of change of TC1 since the year of last treatment is 0.733 cracks/100 ft/year while for TC2 it is 0.233 cracks/100ft/year. TC 3 remained at code zero since the last pavement treatment.

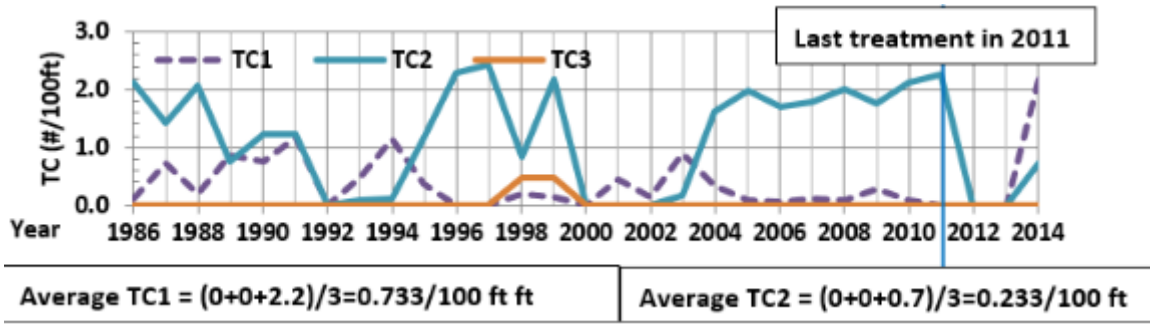

Figure 3.4: Transverse Cracking Codes One (TC1), Two (TC2), and Three (TC3) versus Time for Clay County

Pavement roughness is expressed in terms of International Roughness Index (IRI), the unit of which is in./mile. Code one (1) indicates IRI of less than 105 in./mile; code two (2) indicates IRI that ranges between 105 and 164 in./mile; and for IRI larger than 164 in./mile code three (3) is assigned. IRI value of less than 95 in./mile indicates good roughness condition of pavement (Shahin, 2005). Evolution of IRI for Clay County is depicted in Figure 3.5; thus, resulting in its average rate of change since the last treatment being equal to 61 inch/mile/year.

To characterize the condition of a pavement throughout its depth cores were extracted from pavement at the time of DCP testing. Core locations correspond to DCP locations. Based on the visually assessed level of damage (i.e., missing material, crumbled, cracks, intact, etc.), the

percentage of good, fair, and poor core was calculated as the ratio of the length of a core in good, fair, and poor condition to the total length of a core.

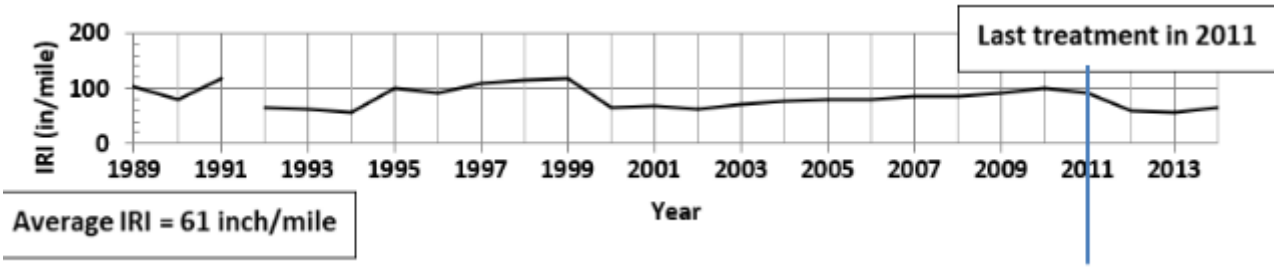

Figure 3.5: IRI versus Time for Clay County

3.4 Predictors

DCP test provides resistance of in situ soil to impact driven penetration. DCP tests were performed on subgrade soils after extracting pavement cores. The test is performed by driving a metal cone into the soil by striking it with 17.6 lb weight dropped from a distance of 2.26 feet. The penetration of the cone after each blow is measured and recorded, thus providing continuous measurements versus depth. KDOT provided DCP results in inch/blow versus depth. KDOT Geotechnical Manual states that DCP results from two top 6-inch intervals should be converted to CBR. To this end, DCP results from 12.5 top inches were used in this study.

KDOT provided the equation based on which the current AADTT can be computed. The equation is given by:

$$\mathbf{TTVGR} = \mathbf{100}\left[\left(\frac{\mathbf{AADTT_{current}}}{\mathbf{AADTT_{initial}}}\right)^{\frac{1}{Current\ map\ year - Initial\ map\ year}} - \mathbf{1}\right]$$

Equation 3.1

Where:

TTVGR = truck traffic volume growth rate

$\mathbf{AADTT_{current}}$ = AADTT in the current year

$\mathbf{AADTT_{initial}}$ = AADT in the initial map year

Current map year and initial map year are self-explanatory. Additional data were provided for all selected pavement sections, including the initial map year and corresponding AADTT, as well as AADTT in the year when DCP tests were conducted. Based on this information, TTVGR can be computed and, thus, AADTT in any year of interest can be computed for the purpose of statistical analyses. Consequently, for Clay County, the average AADTT since the last pavement treatment was used as input into statistical analyses. The average value was computed based on AADTT values for years 2012, 2013, and 2014.

KDOT provided information about pavement layers present in all pavement segments that were selected for the statistical analyses. This information is provided in Appendices A and B of this report. Thickness of unbound layer was provided based on this information and is provided in Table 3.1.

3.5 Results

Four different statistical analyses were employed in this study including:

- Principal Component Regression Analysis (PCRA),
- Regression Analysis (RA),
- Multivariate Principal Component Regression Analysis (MPCRA), and
- Multivariate Regression Analysis (MRA). The analyses were conducted by using statistical software R.

The statistical analyses identified a number of different significant statistical correlations at a level of 0.05 or smaller. In linear regression analysis (including RA, MRA, PCRA, and MPCRA) settings, hypothesis testing can be performed to test statistical significance of the fitted regression model. If the obtained p-value is lower than the α-level (e.g., $\alpha = 0.01$ or $\alpha = 0.05$), then the relationship between the outcome and the predictor is statistically significant. Hence, we can confirm the statistical validity of the fitted regression models.

The results are summarized in Table 3.2, according to which:

- DCP is correlated with total rutting, fatigue cracking code one (FC1), percent of good core, and percent of poor core,
- AADTT is correlated with transverse cracking (TC1 and TC2), and

- thickness of unbound layer is correlated with IRI, percent of good core, and percent of poor core.

Significance levels (α), *p*-values and adjusted R-squared values for each correlation are provided in Table 3.2 along with the relevant type of statistical analysis. Arrows in Table 3.2 indicate the nature of the correlations. Specifically, they show the trends of dependent variables (increasing↑, or decreasing↓) as independent variables in the top row increase (↑).

It is noted that different representations of DCP values are involved in different DCP correlations as indicated in the seventh column of Table 3.2. To this end, values of DCP at depths from zero to 2. 5 inches, from 2.5 to 5 inches, from 5 to 7.5 inches, from 7.5 to 10 inches, and from 10 to 12.5 inches are denoted by DCP1, DCP2, DCP3, DCP4, and DCP5, respectively. Table 3.3 provides further clarification of DCP correlations. Specifically, there are two correlations between the DCP and total rutting rate. PCRA relates total rutting to mean values of DCP1, DCP2, DCP3, DCP4, and DCP5 for each pavement segment. RA relates total rutting rate to mean value of DCP1 only for each pavement segment. Furthermore, fatigue cracking code one (FC1) is correlated with minimum values of DCP1 through DCP5 for each pavement segment, through MPCRA. Finally, the percentage of good core and the percentage of poor core are correlated to each individual value of DCP5 through MRA.

Table 3.2: Summary of Results of Statistical Analyses

Input / Output	DCP ↑	AADTT ↑	Thickness of unbound layer (Th) ↑	Adjusted *R*-squared	Analysis Type	Remarks
Total Rutting (Rt)	$\alpha = 0.01$ $p \leq 0.00696$ ↑	N/A	N/A	0.5473	Principal Component Regression Analysis (PCRA)	21 data points, **mean DCP for each depth**
Total Rutting (Rt)	$\alpha = 0.01$ $p \leq 0.0001$ ↑	N/A	N/A	0.6504	Regression Analysis (RA)	21 data points, **mean DCP1**
Fatigue cracking Code 1 (FC1)	$\alpha = 0.05$ $p = 0.01613$ ↓	N/A	N/A	0.2984	Multivariate Principal Component Regression Analysis (MPCRA)	21 data points, **minimum DCP for each depth**
Transverse Cracking Code 1 (TC1)	N/A	$\alpha = 0.05$ $p = 0.0329$ ↑	N/A	0.1698		21 data points, **minimum DCP** for each depth
Transverse Cracking Code 2 (TC2)	N/A	$\alpha = 0.01$ $p = 0.00243$ ↑	N/A	0.3732		21 data points, **minimum DCP for each depth**
IRI	N/A	N/A	$\alpha = 0.01$ $p \leq 0.0001$ ↓	0.6279		21 data points, **minimum DCP for each depth**
% Good Core (%GC)	$\alpha = 0.01$ $p \leq 0.0001$ ↑	N/A	$\alpha = 0.01$ $p \leq 0.0001$ ↑	0.1590	Multivariate Regression Analysis (MRA)	146 data points, separately considering **DCP 5**
% Poor Core (%PC)	$\alpha = 0.01$ $p \leq 0.00057$ ↓	N/A	$\alpha = 0.01$ $p \leq 0.00057$ ↓	0.1772		

Table 3.3: Details of DCP Correlations

Input / Output	DCP1 ↑	DCP2 ↑	DCP3 ↑	DCP4 ↑	DCP5 ↑	DCP selection	Adjusted R-squared
Total Rutting (Rt) (PCRA)	**Y** ↑	**Y** ↑	**Y** ↑	**Y** ↑	**Y** ↑	**mean DCP** for each depth (21 data points)	0.5473
Total Rutting (Rt) (RA)	**Y** ↑	N	N	N	N	mean DCP1 (21 data points)	0.6504
Fatigue cracking Code 1 (FC1) (MPCRA)	**Y** ↓	**Y** ↓	**Y** ↓	**Y** ↓	**Y** ↓	**min DCP** for each depth (21 data points)	0.2984
% Good Core (%GC) (MRA)	N	N	N	N	**Y** ↑	separately considering **each individual DCP 5** (146 data points)	0.1590
% Poor Core (%PC) (MRA)	N	N	N	N	**Y** ↓	separately considering **each individual DCP 5** (146 data points)	0.1772

3.5.1 PCRA

The correlation between DCP and rate of change of rutting code obtained from PCRA is given by:

$$(\dot{\mathbf{Rt}}) = 0.0443(\overline{\mathbf{DCP1}}) + 0.0474(\overline{\mathbf{DCP2}}) + 0.0563(\overline{\mathbf{DCP3}}) + 0.0566(\overline{\mathbf{DCP4}}) + 0.0511(\overline{\boldsymbol{DCP5}})$$

Equation 3.2

Where:

$\dot{\mathbf{Rt}}$ = average rate of change of rutting severity code (/year) for a given segment since the last treatment

$\overline{\mathbf{DCP1}}$ = mean DCP value (in./blow) in depth zero to 2.5 inches for a given segment

$\overline{\mathbf{DCP2}}$ = mean DCP value (in./blow) in depth 2.5 to 5 inches for a given segment

$\overline{\mathbf{DCP3}}$ = mean DCP value (in./blow) in depth 5 to 7.5 inches for a given segment

$\overline{\mathbf{DCP4}}$ = mean DCP test (in./blow) in depth 7.5 to 10 inches for a given segment

$\overline{\mathbf{DCP5}}$ = mean DCP value (in./blow) in depth 10 to 12.5 inches for a given segment

Equation 3.2 can be interpreted to imply that rutting rate is positively correlated with mean DCP values from depths ranging from zero to 12.5 inches. That is, as mean DCPs increase, rutting code tends to be higher. As shown in Table 3.2 the adjusted *R*-squared value corresponding to Equation 3.2 is 0.5473; thus, implying that 54.73% of rate of change in rutting severity code can be explained by DCP test results.

KDOT uses the correlation between DCP and CBR that is given by Equation 3.3.

$$\ln(\mathbf{CBR}) = 2.37 - 1.12 \ln(\mathbf{DCP})$$

Equation 3.3

Where:

CBR = CBR value (%)

DCP = DCP value (in./blow)

Based on Equation 3.3 the regression model described by Equation 3.2 can be rewritten as:

$$(\dot{Rt}) = (0.0443\ \overline{CBR1}^{-0.8928571} + 0.0474\overline{CBR2}^{-0.8928571} + 0.0563\overline{CBR3}^{-0.8928571} + 0.0566\overline{CBR4}^{-0.8928571} + 0.0511)\ \overline{CBR1}^{-0.8928571})\ \exp(2.116071)$$

Equation 3.4

Where:

$\dot{Rt}$ = average rate of change of rutting severity code (per year) for a given segment since the last treatment

$\overline{CBR1}$ = mean CBR value (in./blow) in depth zero to 2.5 inches for a given segment

$\overline{CBR2}$ = mean CBR value (in./blow) in depth 2.5 to 5 inches for a given segment

$\overline{CBR3}$ = mean CBR value (in./blow) in depth 5 to 7.5 inches for a given segment

$\overline{CBR4}$ = mean CBR test (in./blow) in depth 7.5 to 10 inches for a given segment

$\overline{CBR5}$ = mean CBR value (in./blow) in depth 10 to 12.5 inches for a given segment

Equation 3.4 can be interpreted as average rate of rutting is negatively correlated with mean CBR values from depths ranging from zero to 12.5 inches.

3.5.2 RA

Alternatively, based on RA the rate of change of rutting code can be expressed in terms of average DCP1 value. The corresponding model is given by:

$$(\dot{Rt}) = 0.39843\ (\overline{DCP1})$$

Equation 3.5

Where:

$\dot{Rt}$ = average rate of change of rutting severity code (per year) for a given segment since the last treatment

$\overline{DCP1}$ = mean DCP value (in./blow) in depth zero to 2.5 inches for a given segment

Equation 3.5 can be interpreted to imply that rutting is positively correlated with $\overline{\text{DCP1}}$. That is as $\overline{\text{DCP1}}$ increases rutting code tends to be higher. Furthermore, adjusted *R*-squared value corresponding to Equation 3.5 is 0.6504, thus implying that 65.04% of rutting can be explained by $\overline{\text{DCP1}}$.

Equation 3.5 can be modified with the aid of Equation 3.3., thus obtaining:

$$(\dot{Rt}) = 0.39843\ (\overline{CBR1})^{-0.8928571}\ \exp(2.116071)$$

Equation 3.6

Where:

$\dot{Rt}$ = average rate of change of rutting severity code (per year) for a given segment since the last treatment

$\overline{CBR1}$ = mean CBR value (in./blow) in depth zero to 2.5 inches for a given segment

Equation 3.6 indicates that the smaller the average CBR value from depth of zero to 2.5 inches, the larger the average rate of change of rutting severity code.

3.5.3 MPCRA

Four different statistical models were obtained from MPCRA. The first model correlates DCP values to fatigue cracking code one (FC1). The corresponding correlation is given by:

$$\overline{FC1} = 3.3019644 - 0.4032331(DCP1_{min}) - 0.4709366(DCP2_{min}) - 0.7212926(DCP3_{min}) - 0.8149346(DCP4_{min}) - 0.7292693(DCP5_{min})$$

Equation 3.7

Where:

$\overline{FC1}$ = average value of fatigue cracking code (ft/100ft/year) one (1) for a given segment since the last treatment

$DCP1_{min}$ = minimum DCP value (in./blow) in depth zero to 2.5 inches for a given segment

$DCP2_{min}$ = minimum DCP value (in./blow) in depth 2.5 to 5 inches for a given segment

$DCP3_{min}$ = minimum DCP value (in./blow) in depth 5 to 7.5 inches for a given segment

$DCP4_{min}$ = minimum DCP value (in./blow) in depth 7.5 to 10 inches for a given segment

$DCP5_{min}$ = minimum DCP value (in./blow) in depth 10 to 12.5 inches for a given segment

Equation 3.7 indicates that, as a minimum DCP in depths ranging from zero to 12.5 inches decreases, the fatigue cracking code one tends to be higher. The corresponding adjusted *R*-squared

value is 0.2984; thus, implying that 29.84% of fatigue cracking code one can be explained by DCP test results. Although this finding appears counterintuitive at first, it is noted that it was found that DCP test results are correlated with fatigue cracking code one only. Therefore, no statistically significant correlations were found between DCP values and fatigue cracking codes two, three, or four. Consequently, this finding can be interpreted to imply that minimum DCP values for a given pavement segment were found to be negatively correlated to the initiation of fatigue cracking.

The second model correlates transverse cracking code one (TC1) with the truck traffic volume (AADTT). The corresponding equation is given by:

$$\overline{TC1} = 0.2836606 + 0.0001409\ (\overline{AADTT})$$

Equation 3.8

Where:

$\overline{TC1}$= average transverse cracking code one (1) (no. of cracks/100ft) for a given segment since the last treatment

$\overline{AADTT}$= average annual daily truck traffic (no. of trucks/day) since the last treatment

Equation 3.8 indicates that as average AADTT increases, average transverse cracking code one (TC1) tends to increase. In addition, the adjusted *R*-squared value is 0.1698 for this correlation. Thus, 16.98% of transverse cracking code one can be explained by the truck traffic volume (AADTT).

The third model correlates transverse cracking code two (TC2) with the truck traffic volume. The corresponding equation is given by:

$$\overline{TC2} = 0.0319144 + 0.0000854(\overline{AADTT})$$

Equation 3.9

Where:

$\overline{TC2}$ = average transverse cracking code two (2) (no. of cracks/100ft) for a given segment since the last treatment

$\overline{AADTT}$= average annual daily truck traffic (no. of trucks/day) since the last treatment

Equation 3.9 indicates that as the average AADTT increases, average transverse cracking code two (TC2) tends to increase. In addition, the adjusted *R*-squared value is 0.3732 for this

correlation. Therefore, 37.32% of transverse cracking code one can be explained by truck traffic volume (AADTT).

Both equations Equation 3.8 and Equation 3.9 may appear counterintuitive at first. Specifically, transverse cracking is thought to be primarily thermally induced. Nevertheless, it is noted that AADTT was not found to be correlated with transverse cracking code zero (TC0), and thus not to the initiation of transverse cracking. The finding that daily truck traffic may affect evolution of transverse cracking after it has been thermally initiated seems to be reasonable.

The fourth model correlates pavement roughness and thickness of unbound layer. The corresponding equation is given by:

$$\overline{IRI} = 53.4082348 - 7.62793\ (Th)$$

Equation 3.10

Where:

$\overline{IRI}$ = average value of international roughness index (in/mile) since the last pavement treatment

Th = thickness of unbound layer (in.)

The adjusted *R*-squared value that corresponds to Equation 3.9 is 0.6279; thus, implying that 62.79% of average IRI can be explained by thickness of unbound layer. Consequently, average IRI is negatively correlated with thickness of unbound layer.

3.5.4 MRA

The number of DCP tests for each pavement segment used in this analysis is listed in Table 3.4; thus, adding up to a total of 146 for all selected segments.

Table 3.4: Observations Collected for MRA

No.	County	Lane	Number of DCP tests/cores
1	CHEROKEE	EB	11
2	CHEROKEE	WB	12
3	CLAY	EB	10
4	CLAY	WB	11
5	DOUGLAS	EB	7
6	DOUGLAS	WB	10
7	FORD	EB	3
8	FORD	WB	3
9	GOVE	EB	9
10	GOVE	WB	6
11	HARPER	EB	5
12	HARPER	WB	4
13	JOHNSON3	NB	5
14	JOHNSON3	SB	5
15	RENO	EB	13
16	RENO	WB	7
17	SHAWNEE1	EB	3
18	SHAWNEE1	WB	2
19	SHAWNEE2	WB	2
20	THOMAS	EB	8
21	THOMAS	WB	10

The first MRA model that resulted from this analysis is given by:

$$\ln (GC + 1) = 0.218686 + 0.116029(DCP5) + 0.031956(Th)$$

Equation 3.11

Where:

GC = amount of good core (%/100)

DCP5 = individual DCP value (in./blow) in depth 10 to 12.5 inches

Th = thickness of unbound layer (inch)

The corresponding adjusted *R*-squared value is 0.159 thus implying that 15.90% of good core can be explained by the value of DCP5 and thickness of unbound layer. The second MRA model is described by:

$$\ln (PC + 1) = 0.430204 - 0.127968 (DCP5) - 0.036959(Th)$$

Equation 3.12

Where:

PC = amount of good core (%/100)

DCP5 = individual DCP value (in./blow) in depth 10 to 12.5 inches

Th = thickness of unbound layer (inch)

The corresponding adjusted *R*-squared value is 0.1772, thus implying that 17.72% of poor core can be explained by the value of DCP5 and thickness of unbound layer. Equations 3.11 and 3.12 imply that as DCP5 increases or CBR5 decreases the percentage of good quality core tends to increase while the percentage of the bad quality core decreases. Furthermore, as the thickness of unbound layer increases the percentage of good quality core in the analysis tends to be higher while the percentage of bad quality core decreases. The effect of the thickness of unbound layer is as expected. The effect of DCP5 value on percent of good and poor core may appear counterintuitive at first. Nevertheless, it is in agreement with the correlation between mean values of DCP1 through DCP5 with fatigue cracking code one (FC1) that was obtained from MPCRA. An increase in a minimum DCP value within a given pavement segment essentially appears to shift the location of damage from initiation of fatigue cracking to increase in total rutting. Specifically, an increase in minimum DCP indicates a weaker and less stiff, but more uniform subgrade. Consequently, if there is less fatigue cracking there will be a decreased amount of poor core and likely the increased amount of good core.

Four additional statistical models were considered in this group to evaluate the importance of each predictor in the regression models. The additional models consider only DCP5 or only thickness of unbound layer as predictors for the percent of good core and percent of poor core. The corresponding values of adjusted *R*-squared are provided in Table 3.5.

Table 3.5: Comparison of Adjusted *R*-squared Values for Different Predictors

Outcome	Used Predictors	Adjusted *R*-squared
Good Core (%)	DCP5 & Thickness	0.159
Poor Core (%)	DCP5 & Thickness	0.1772
Good Core (%)	DCP5	**0.04271**
Poor Core (%)	DCP5	**0.04364**
Good Core (%)	Thickness	0.0964
Poor Core (%)	Thickness	0.1119

It is noted that the exclusion of thickness from the models listed in Table 3.5 leads to a larger decrease in adjusted *R*-squared than the exclusion of DCP5. This implies that thickness of unbound layer has a stronger effect on core analysis than DCP5.

Chapter 4: Applications and Implementations

In this section several graphs that represent correlations with DCP and CBR are depicted.

4.1 Rutting

Because the regression model given by Equation 3.5 provides mean rate of change in the rutting severity code in terms of mean DCP1 value, the time interval corresponding to the unit increase in rutting severity code can be predicted. The corresponding equation is given by:

$$t_{u\text{-}rutt} = \frac{1}{0.3984327(\overline{DCP1})}$$

Equation 4.1

Where:

$t_{u\text{-}rutt}$ = time interval (yr) corresponding to the unit increase in rutting code since the last treatment

$\overline{DCP1}$ = mean value of DCP (in./blow) in depth zero to 2.5 inches for a given segment

Graphical representation of Equation 3.11 is shown in Figure 4.1. Both Equation 4.1 and Figure 4.1 can be used to determine an acceptable DCP value within the top one inch of a subgrade soil.

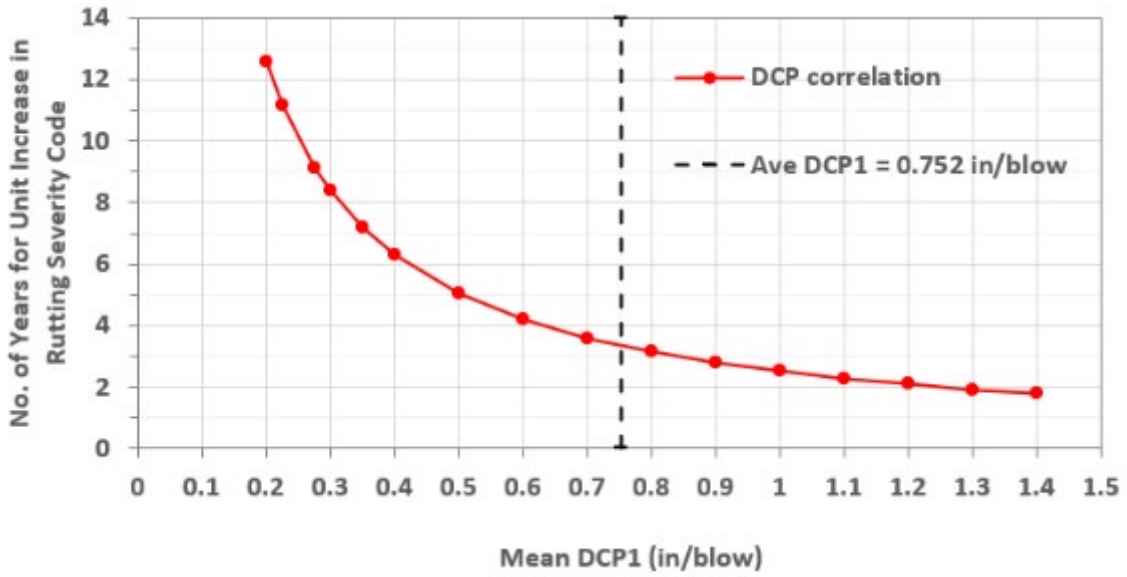

Figure 4.1: Time since the Last Treatment Required for Unit Increase in Rutting Severity Code versus Average DCP1

It is noted that the average DCP1 value for all pavement segments considered in this study is 0.752 in./blow. The RA model predicts that it would take 3.34 years for the unit increase in the rutting severity code at mean DCP1 value of 0.752 in./blow.

Equation 4.1 can be reformulated into Equation 4.2 with the aid of Equation 3.3. The resulting equation is given by:

$$t_{u\text{-}rutt} = \frac{\overline{CBR1}^{0.8928571}}{0.3984327\ exp(2.116071)}$$

Equation 4.2

Where:

$t_{u\text{-}rutt}$ = time interval (yr) corresponding to unit increase in rutting code since the last treatment

$\overline{CBR1}$ = mean value of CBR (%) in depth zero to 2.5 inches for a given segment

Equation 4.2 is depicted in Figure 4.2. The average CBR value for the top 2.5 inches for all pavement segments considered in this study is 14.72 percent. According to Figure 4.2 and Equation 4.2, 3.34 years is required for the unit increase in the rutting severity code at the mean CBR value of 14.72 percent. Figure 4.2 and Equation 4.2 provide helpful tools for selecting an acceptable CBR1 value.

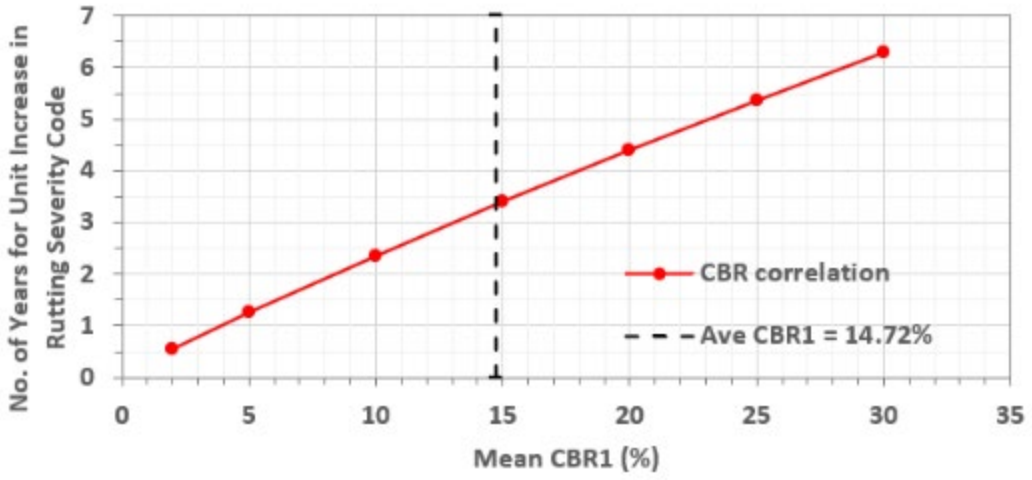

Figure 4.2: Time since the Last Treatment Required for Unit Increase in Rutting Severity Code versus Average CBR1

4.2 Core Quality

Next, the percentage of good, poor, and fair cores are expressed in terms of DCP5 and thickness of unbound layer according to the results of MRA. Equation 3.11 is presented in graphical form in Figure 4.3, which can be helpful when deciding about acceptable values of DCP5.

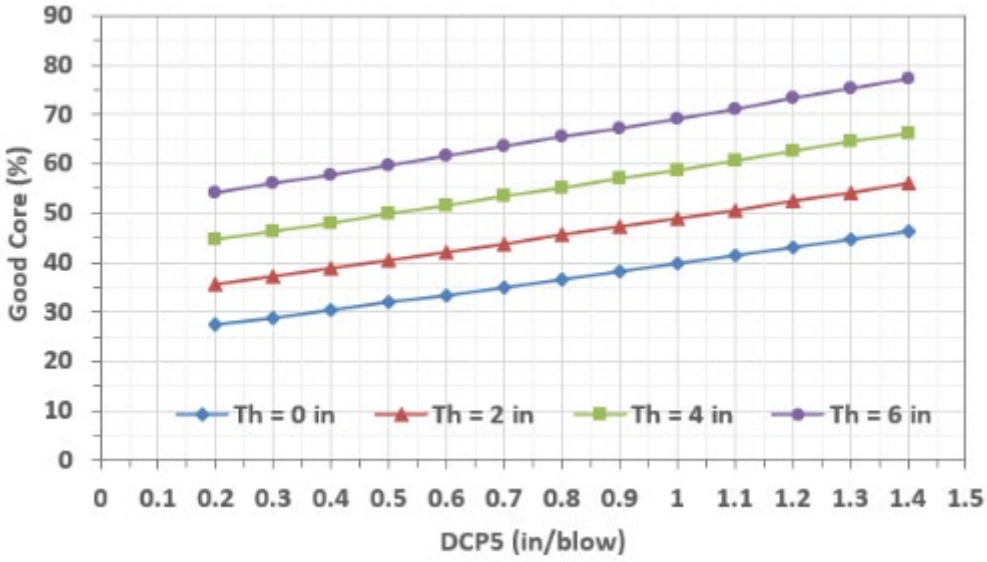

Figure 4.3: Percentage of Good Core versus DCP5 for Different Thicknesses of Unbound Layer

The percentage of poor core for different thicknesses of unbound layer can be obtained from Equation 3.12. The corresponding graph is depicted in Figure 4.4.

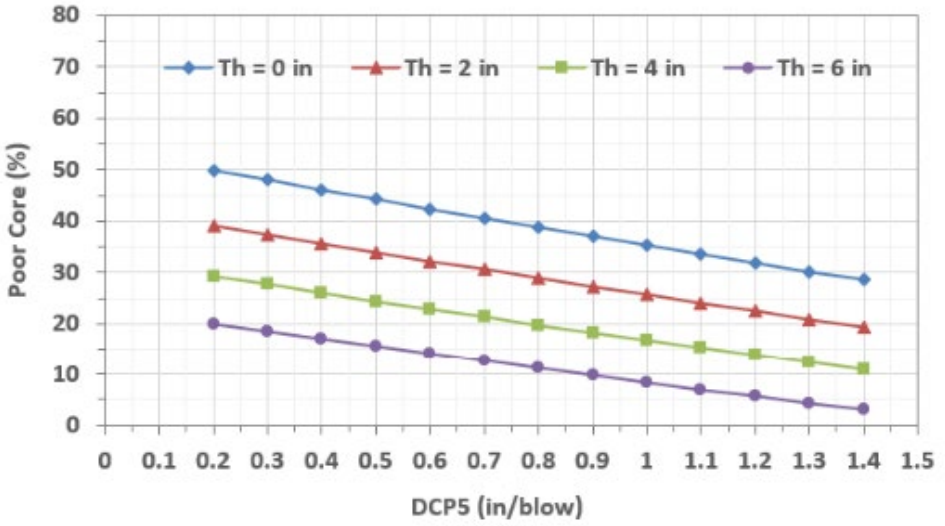

Figure 4.4: Percentage of Poor Core versus DCP5 for Different Thicknesses of Unbound Layer

The percentage of core in fair condition can simply be obtained by subtracting the sum of percentages of good and poor cores from 100%. The corresponding graph is depicted in Figure 4.5.

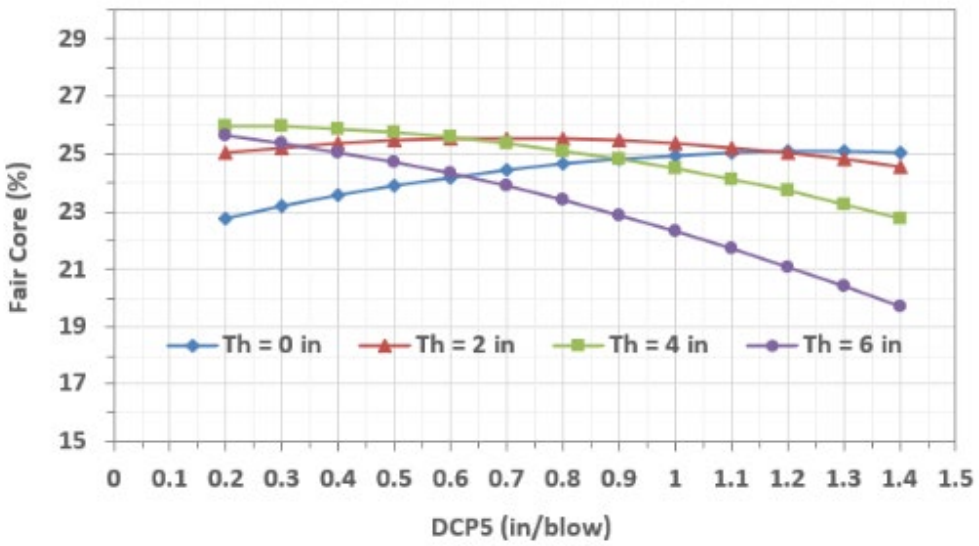

Figure 4.5: Percentage of Fair Core versus DCP5 for Different Thicknesses of Unbound Layer

Alternatively, DCP can be expressed in terms of CBR according to Equation 3.3. Combining Equation 3.3 with Equation 3.11 results in:

$$GC(\%) = 100\,[\exp(0.218686 + 0.962863\,(CBR5)^{(-0.892857)} + 0.031956\,(Th)) - 1]$$

Equation 4.3

With:

GC (%) = percent of good core

CBR5 = CBR value (%) in depth 10 to 12.5 inches for a given segment

Th = thickness of unbound layer (in.)

Equation 4.3 is shown in graphical form in Figure 4.6 that can be useful when determining the acceptable value of CBR5.

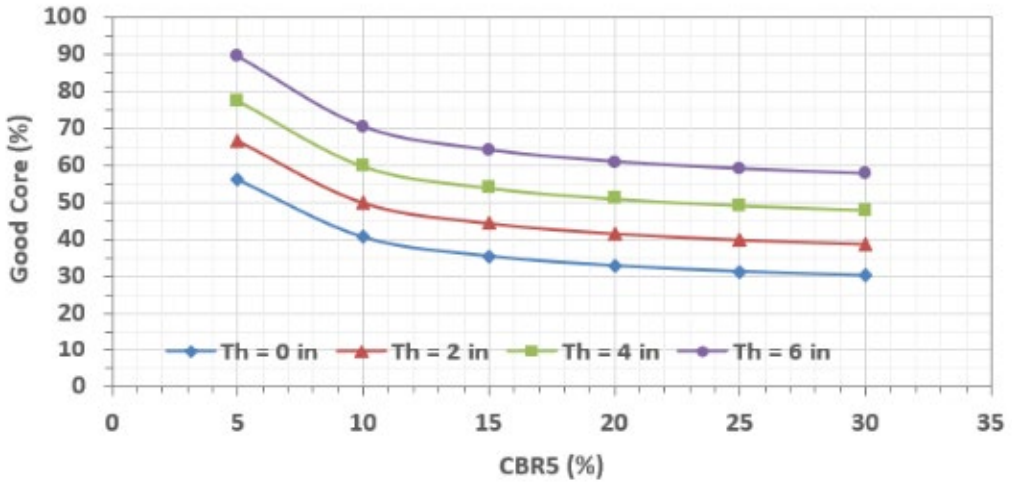

Figure 4.6: Percentage of Good Core versus CBR5 for Different Thicknesses of Unbound Layer

Similarly, Equation 3.12 can be modified with the aid of Equation 3.3. The resulting equation is given by:

$$PC(\%) = 100\,[\exp(0.430204 - 1.061939\,(CBR5)^{(-0.892857)} - 0.036959(Th))-1]$$

Equation 4.4

With:

PC (%) = percent of poor core

CBR5 = CBR value (%) in depth 10 to 12.5 inches for a given segment

Th = thickness of unbound layer (in.)

Equation 4.4 is shown in graphical form in Figure 4.7 that can be useful when determining the acceptable value of CBR5.

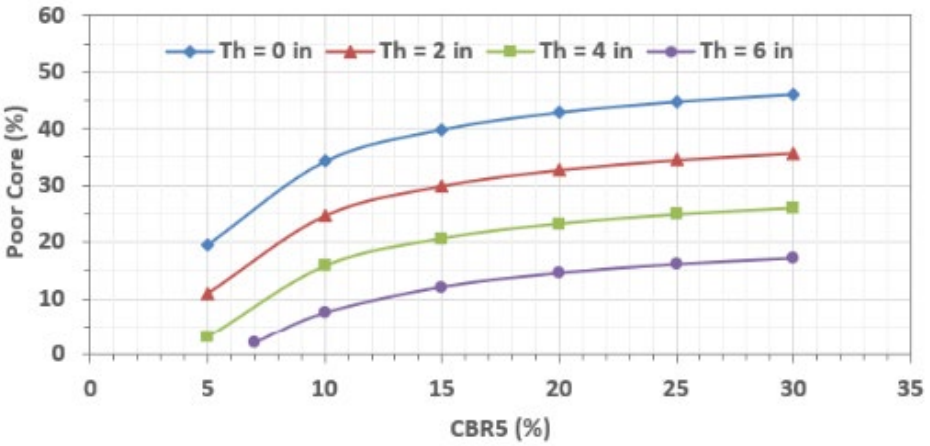

Figure 4.7: Percentage of Poor Core versus CBR5 for Different Thicknesses of Unbound Layer

Finally, the percentage of core in fair condition can be obtained by subtracting the sum of percentage of good and poor core from one hundred. The corresponding graph is depicted in Figure 4.8.

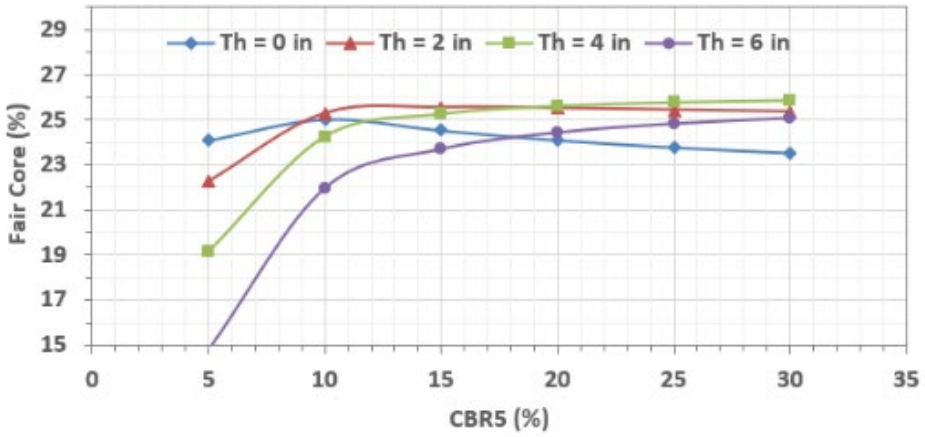

Figure 4.8: Percentage of Fair Core versus CBR5 for Different Thicknesses of Unbound Layer

Figures 4.6, 4.7, and 4.8 can be helpful with determining the acceptable value of CBR. Based on these figures, it is noted that the largest magnitude of change in the percentage of good, poor, and fair cores that occurs is smaller than 10% for CBR5. The changes in the percentage of good and poor cores between CBR5 values of 10% and 15% are about the same as the changes between the values of 15% and 30% for CBR5. Thus, the rate of change in percentage of good and poor cores slows down as CBR increases.

Chapter 5: Discussion

It is noted that the results in this study were obtained by statistical analyses of in-service pavements based on the collected distress data and collected values of predictor variables. Furthermore, this study is focused primarily on the effects of subgrade on distresses of flexible pavements in Kansas. Hence, the most relevant findings are those related to the effects of DCP test results (or CBR values) on pavement distress. They are discussed first.

5.1 DCP Correlations

One of the major findings in this study is that increase in the mean DCP value, or decrease in CBR, causes increase in total rutting. Two different analyses resulted in this finding. Specifically, a mean DCP value for each 2.5 inch depth segment, up to a total of 12.5 inches, is positively correlated with the average rate of change of rutting severity code according to PCRA. The mean DCP value within only 2.5 top inches of subgrade is positively correlated with the average rate of change of rutting severity code, according to RA. A mean value refers to the average of all DCP tests performed on a given pavement segment. In summary, the larger the mean DCP value (or the smaller the CBR) the more total rutting is expected.

CBR is often correlated with resilient modulus of subgrade (M_R). For example, KDOT (2007) uses the following correlation:

$$\mathbf{M_R = 800(CBR)} \qquad \textbf{Equation 5.1}$$

Where:

M_R = resilient modulus (psi) of subgrade soil

CBR = California Bearing Ratio (%)

Thus, according to Equation 5.1 resilient modulus is directly proportional to CBR. In other words, as resilient modulus increases so does the CBR while the corresponding DCP value decreases.

The second finding related to DCP is that increase in minimum DCP value for each of top five 2.5 inches depth segments of subgrade is negatively correlated to fatigue cracking code one (FC1). Thus, the larger the minimum DCP value within each 2.5 inch depth segment the smaller

fatigue cracking code one is expected. Specifically, the weaker or the less stiff the subgrade is at the location where it is the strongest (minimum DCP) within the given pavement segment, the less likely is the fatigue cracking to initiate. This may imply that the increasing amount of subgrade uniformity with respect to its stiffness and strength decreases the probability that the fatigue cracking will be initiated.

The third finding related to DCP test is that the higher the individual DCP value at a depth of subgrade between 10 and 12.5 inches the higher the percent of good core and the lower the percent of poor core at the same location. This finding seems to agree with the previous one related to fatigue cracking as less initiation of fatigue cracking would likely increase the percent of good core and decrease the percent of poor core.

Schwartz, Li, Ceylan, S. Kim, and Gopalakrishnan (2013) performed global sensitivity analyses of mechanistic-empirical performance predictions for flexible pavements by using multivariate linear regression analysis and artificial neural networks. They used traffic volume (AADTT), thickness of different pavement layers, and material properties of different layers including the resilient modulus of subgrade soil as design inputs. They found that all pavement distresses are hypersensitive to the hot-mix asphalt (HMA) layer properties. Schwartz et al. (2013) also found that longitudinal and alligator cracking are very sensitive to the resilient modulus of subgrade. Their finding indicates that increase in the resilient modulus of subgrade (M_R) leads to decrease in alligator and longitudinal cracking, which at least partially disagrees with the finding from this report related to the initiation of fatigue cracking. Furthermore, Schwartz et al. (2013) did not find that either total rutting or AC rutting is sensitive to the resilient modulus of subgrade, which is also in disagreement with the related finding herein.

Shahji (2006) conducted sensitivity analysis of AASHTO 2002 design guide for flexible and rigid pavements. Various design parameters including traffic loads, thicknesses, and moduli of different pavement layers were considered in the analysis. Shahji (2006) found that increase in subgrade modulus induces increase in fatigue cracking in flexible pavements, which agrees with the related finding in this study.

5.2 AADTT Correlations

In this study, only two pavement distresses turned out to be correlated to AADTT. They are transverse cracking code one (TC1) and transverse cracking code two (TC2). As explained previously transverse cracking code zero (TC0) can be interpreted as initiation of transverse cracking. Thus, initiation of transverse cracking was not found to be related to AADTT, but rather the evolution of transverse cracking, which is accelerated by increase in AADTT.

Schwartz et al. (2013) for example, found that thermal cracking was very sensitive to the modulus, tensile strength, and creep compliance of HMA. The effects of AC on pavement distresses were not included in this study as the primary emphasis was on the effects of subgrade, and secondary on the effects of unbound layer and traffic volume.

In this study, it was not found that AADTT is correlated with total rutting. Similarly, Rahman (2017) found that Average Annual Daily Traffic (AADT) had no significant influence on rutting.

5.3 Thickness of Unbound Layer

In this study, thickness of unbound layer was found to be correlated to roughness of pavement. The larger the thickness the smaller the IRI. Masad and Little (2004), who conducted sensitivity analyses of AASHTO 2002 Model, reported a similar finding. They found that base modulus and thickness have a significant influence on the IRI and longitudinal cracking. They also found that base properties have almost no influence on permanent deformation.

In this study, DCP was not found to have statistically significant correlation with IRI. Similarly, Shahji (2006) found that using larger subgrade modulus did not reduce IRI. Shahji (2006) also found that base properties have no influence on permanent deformation of pavement. In addition, thickness of unbound layer was also found to be correlated with the percentage of good core and the percentage of poor core in this study.

5.4 Adjusted *R*-squared Values

Adjusted *R*-squared values for different statistically significant correlations were provided in Table 3.2. It is noted that the rutting correlation obtained from RA has the highest adjusted *R*-squared (0.6504), which is followed by the IRI correlation (adjusted R^2 = 0.6279) obtained from

MPCRA. The next one is the other rutting correlation (adjusted $R^2 = 0.5473$) obtained from PCRA. These are followed by transverse cracking code two (adjusted $R^2 = 0.3732$), fatigue cracking code one (adjusted $R^2 = 0.2984$), percent of poor core (adjusted $R^2 = 0.1772$), transverse cracking code 1 (adjusted $R^2 = 0.1698$), and finally percent of good core (adjusted $R^2 = 0.1590$). Similarly, Schwartz et al. (2013) found from multivariate linear regression analysis that rutting and IRI distresses tend to have relatively better goodness-of-fit statistics while longitudinal and alligator cracking tend to have smaller *R*-squared values.

Chapter 6: Conclusions and Recommendations

6.1 Conclusions

Multiple statistical analyses were performed to arrive at scientifically based recommendation for acceptable CBR values for flexible pavements in the state of Kansas. Different statistical models were employed to predict pavement performance. Primary emphasis in these analyses was on effects of subgrade soil on pavement distresses, while secondary emphasis was on the effects of thickness of unbound layer and traffic volume. The predicted distresses included: 1) total rutting, 2) fatigue cracking, 3) transverse cracking, 4) pavement roughness, and 5) pavement core condition.

The statistically significant correlations that involve DCP or CBR are the correlations between DCP and total rutting, DCP and fatigue cracking code one (FC1), DCP and the percentage of good core, and DCP and the percentage of poor core. All correlations are functions of a single variable, except the percentages of good and poor core, which depend on both DCP value and thickness of unbound layer. To help with selection of acceptable CBR values two sets of x-y graphs have been constructed. In the first set, there is only one graph that provides the number of years needed to increase rutting code by one unit versus DCP or CBR value. The second set of graphs shows the percentage of good, poor, and fair cores versus DCP or CBR values for different thicknesses of unbound layer. In addition to these graphs, the correlation equations that relate fatigue cracking code one (FC1) and alternative relationship for rutting, which relates the average rutting rate to DCP values from the top 12.5 inches of subgrade, can be used when determining the acceptable CBR value.

6.2 Recommendations

In this section, the specific equations and graphs that can be used to determine acceptable value of CBR for flexible pavements in Kansas are described.

Equations 3.2 and 3.4 provide the average rate of rutting severity code change in terms of average values of DCP test results and corresponding average CBR values, respectively. In this case DCP test results within the top 12.5 inches of subgrade soil are needed. Equations 3.5 and 3.6 provide an average rutting severity code rate in terms of average DCP test results and

corresponding CBR values within the top 2.5 inches of subgrade only. Based on Equations 3.5 and 3.6 additional graphs, which are presented in Figures 4.1 and 4.2, were constructed. These graphs provide the number of years needed for the unit increase in the rutting severity code versus the average DCP1 and average CBR1 value, respectively. Furthermore, Equations 4.1 and 4.2 describe the curves depicted in Figures 4.1 and 4.2.

Equation 3.7 provides average fatigue cracking code one (FC1) as a function of minimum of individual DCP values throughout the top 12.5 inches of subgrade soil. Equations 3.11 and 3.12 provide the amount of good core and poor core, respectively, as a function of individual DCP5 values and thickness of unbound layer. Figures 4.3, 4.4, and 4.5 provide percent of good core, poor core, and fair core, respectively, as a function of DCP5 and thickness of unbound layer. Alternatively, Equations 4.3 and 4.4 provide amount of good core and poor core as function of CBR5 and thickness of unbound layer. Figures 4.6, 4.7, and 4.8 depict amount of good core, poor core and fair core as a function of CBR5 and thickness of unbound layer.

Apart from DCP correlations, additional statistically significant correlations were found in this study. Equations 3.8 and 3.9 provide the average value of thermal cracking codes one and two (TC1 and TC2) as functions of the average value of AADTT. Finally, Equation 3.10 provides average value of roughness (IRI) as a function of thickness of unbound layer.

6.3 Future Work

It would be useful to expand the current statistical analyses by including weather data. Specifically, average annual temperature and precipitation could be included together with predictors and predicted distresses. In addition, the statistical analyses could possibly be expanded further back in time to include pavement distresses prior to the last pavement treatment. These analyses could also evaluate effectiveness of different types of pavement treatments that were applied prior to the last treatment and contribute towards better planning of pavement management operations.

References

American Association of State Highway and Transportation Officials (AASHTO). (2008). *Mechanistic-empirical pavement design guide: A manual of practice*. AASHTO.

Baus, R. L., & Stires, N. R. (2010). Mechanistic-empirical pavement design guide *(MEPDG) implementation* (Report No. FHWA-SC-10-01). University of South Carolina. https://rosap.ntl.bts.gov/view/dot/25115

Chan, P. K., Oppermann, M. C., & Wu, S.-S. (1997). North Carolina's experience in development of pavement performance prediction and modeling. *Transportation Research Record*, *1592*, 80–88. https://doi.org/10.3141/1592-10

DeLisle, R. R., Sullo, P., & Grivas, D. A. (2003). Network-level pavement performance prediction model incorporating censored data. *Transportation Research Record: Journal of the Transportation Research Board*, *1853*, 72–79. https://doi.org/10.3141/1853-09

Henning, T. F. P., Costello, S. B., Dunn, R. C. M., Parkman, C. C., & Hart, G. (2004). The establishment of a long-term pavement performance study on the New Zealand State Highway Network. *Road and Transport Research*, *13*(2), 17–32. https://www.proquest.com/scholarly-journals/establishment-long-term-pavement-performance/docview/215248021/se-2

Isa, A. H. M., Ma'soem, D. M., & Hwa, L. T. (2005). Pavement performance model for federal roads. *Proceedings of the Eastern Asia Society for Transportation Studies*, *5*, 428–440. https://www.easts.info/on-line/proceedings_05/428.pdf

Johnson, K. D., & Cation, K. A. (1992). Performance prediction development using three indexes for North Dakota pavement management system. *Transportation Research Record*, *1344*, 22–30. https://onlinepubs.trb.org/Onlinepubs/trr/1992/1344/1344-004.pdf

Kansas Department of Transportation (KDOT). (2007). *Geotechnical manual*. KDOT.

Kim, S.-H., & Kim, N. (2006). Development of performance prediction models in flexible pavement using regression analysis method. *KSCE Journal of Civil Engineering*, *10*(2), 91–96. https://doi.org/10.1007/BF02823926

Luo, X., Gu, F., Zhang, Y., Lytton, R. L., & Zollinger, D. (2017). Mechanistic-empirical models for better consideration of subgrade and unbound layers influence on pavement performance. *Transportation Geotechnics*, *13*, 52-68. https://doi.org/10.1016/j.trgeo.2017.06.002

Madanat, S. (1993). Incorporating inspection decisions in pavement management. *Transportation Research Part B: Methodological*, *27*(6), 425–438. https://doi.org/10.1016/0191-2615(93)90015-3

Masad, S. A., & Little, D. N. (2004). *Sensitivity analysis of flexible pavement response and AASHTO 2002 design guide to properties of unbound layers* (Report No. ICAR 504-1). International Center for Aggregates Research, University of Texas at Austin. http://hdl.handle.net/2152/35370

Meegoda, J. N., & Gao, S. (2014). Roughness progression model for asphalt pavements using long-term pavement performance data. *Journal of Transportation Engineering*, *140* (8). https://doi.org/10.1061/(ASCE)TE.1943-5436.0000682

Mills, L. N. O., Attoh-Okine, N. O., & McNeil, S. (2012). Developing pavement performance models for Delaware. *Transportation Research Record: Journal of the Transportation Research Board*, *2304*, 97–103. https://doi.org/10.3141/2304-11

Orobio, A., & Zaniewski, J.P. (2011). Sampling-based sensitivity analysis of the *Mechanistic-empirical pavement design guide* applied to material inputs. *Transportation Research Record: Journal of the Transportation Research Board*, *2226*, 85-93. https://doi.org/10.3141/2226-09

Prozzi, J. A., & Madanat, S. M. (2004). Development of pavement performance models by combining experimental and field data. *Journal of Infrastructure Systems*, *10*(1), 9-22. https://doi.org/10.1061/(ASCE)1076-0342(2004)10:1(9)

Puppala, A. J., Saride, S., & Chomtid, S. (2009). Experimental and modeling studies of permanent strains of subgrade soils. *Journal of Geotechnical and Geoenvironmental Engineering, 135*(10), 1379–1389. https://doi.org/10.1061/(ASCE)GT.1943-5606.0000163

Rahman, M. M. (2017). *Characterization of subgrade resilient modulus for MEPDG and the effects on pavement rutting* (Doctoral dissertation). University of South Carolina. https://scholarcommons.sc.edu/etd/4383

Schwartz, C. W., Li, R., Ceylan, H., Kim, S., & Gopalakrishnan, K. (2013). Global sensitivity analysis of mechanistic-empirical performance predictions for flexible pavements. *Transportation Research Record: Journal of the Transportation Research Board, 2368*, 12–23. https://doi.org/10.3141/2368-02

Shahin, M. Y. (2005). *Pavement management for airports, roads, and parking lots* (2nd ed.). Springer.

Shahji, S. (2006). *Sensitivity analysis of AASHTO's 2002 flexible and rigid pavement design methods* (Master's thesis). University of Central Florida. https://stars.library.ucf.edu/cgi/viewcontent.cgi?article=2061&context=etd

Waseem, A., & Yuan, X.-X. (2013). Longitudinal local calibration of MEPDG permanent deformation models for reconstructed flexible pavements using PMS data. *International Journal of Pavement Research and Technology*, *6*(4), 304-312. https://www.researchgate.net/profile/Afzal-Waseem/publication/258021502

Appendix A: Layering and Cross Sections of Selected Pavement Segments

Appendix A contains graphical representations of historical record of pavement layers and cross sections of the selected pavement segments.

The KDOT project number for Cherokee County is 166-11 KA 3905-01. It extends from 0.2 miles east of east junction US-50/US-283 northeast to 1.0 mile east of RS-257 and RS-1165, east to 4.2 miles of RS0-1165. A total current thickness of the pavement is 19.75 inches and length of the segment is 4.297 miles. Historical record of layers is depicted in Figure A.1, while the cross section of this pavement segment is depicted in Figure A.2.

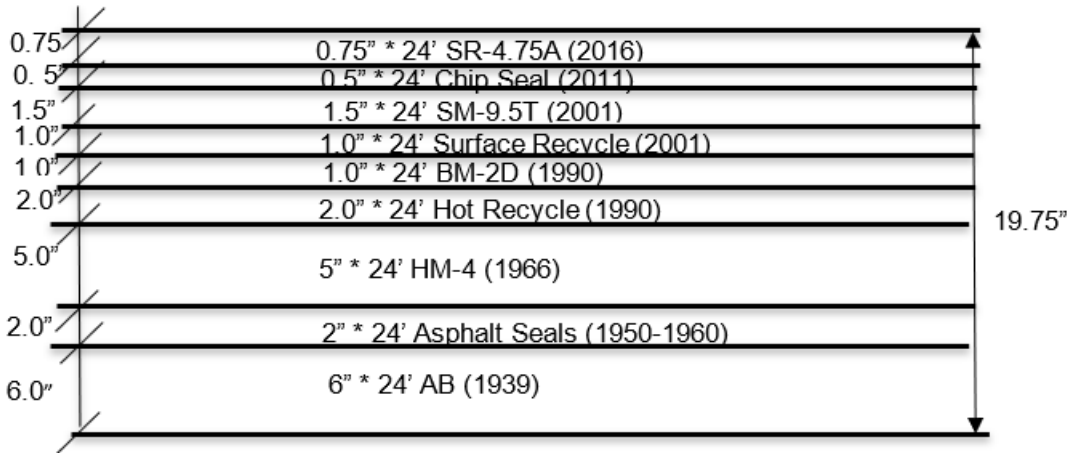

Figure A.1: Historical Record of Pavement Layers in Cherokee County

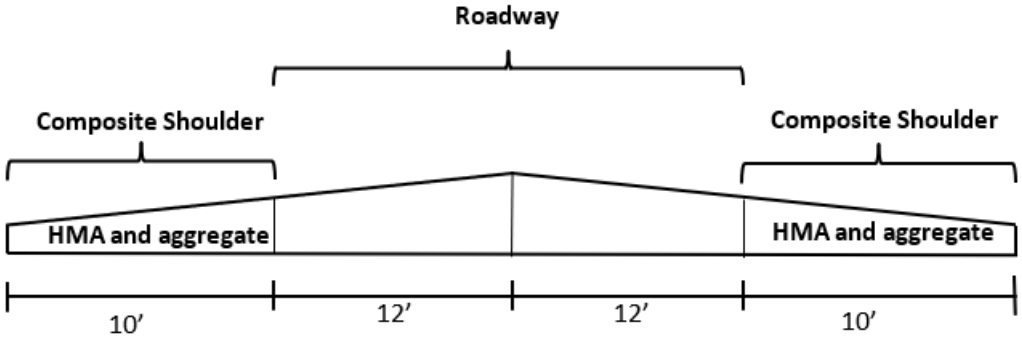

Figure A.2: Cross Section of Pavement in Cherokee County

All abbreviations used in figures in Appendix A are explained in Appendix B.

The KDOT project number for Clay County is 24-14 KA 3240-01. The first segment extends from Clay/Cloud County line east to RS 1408. Its total length is 6.935 miles, and its current total thickness is 17.3 inches. A historical record of layers is depicted in Figure A.3, while the cross section of this segment is shown in Figure A.4.

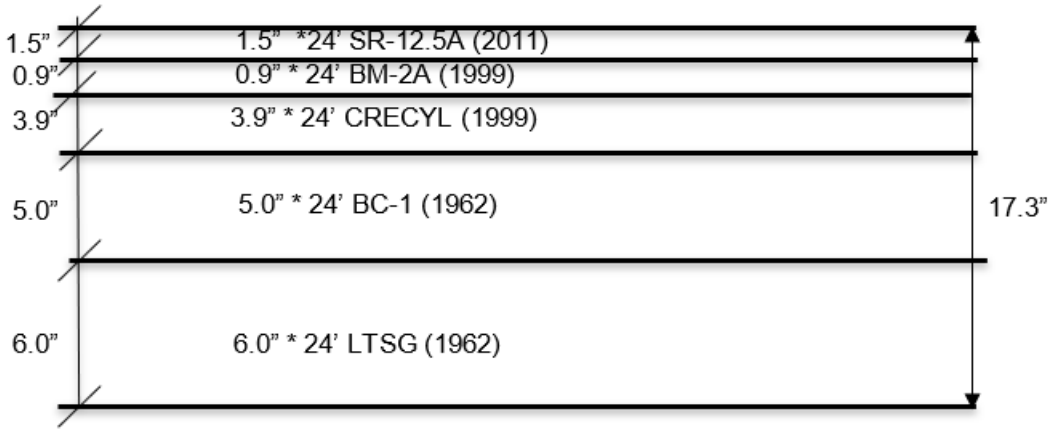

Figure A.3: Historical Record of Pavement Layers in Clay County, Segment One

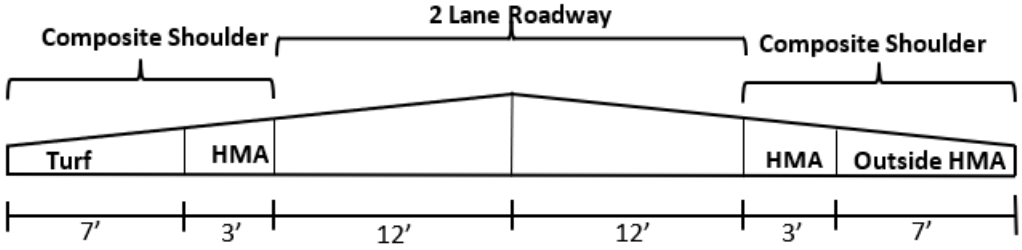

Figure A.4: Cross Section of Pavement in Clay County, Segment One

The second segment in Clay County extends from RS 1408 east to 2.935 mi east of RS 1408. The current total thickness of this segment is 14.3 inches, and its length is 2.935 miles. The layering is depicted in Figure A.5.

The third segment in Clay County extends from 2.935 miles east of RS 1408, east to 3.896 miles east of RS 1408. Currently, the total thickness is 16.9 inches and length of the segment is 0.961 miles. The layering is depicted in Figure A.6.

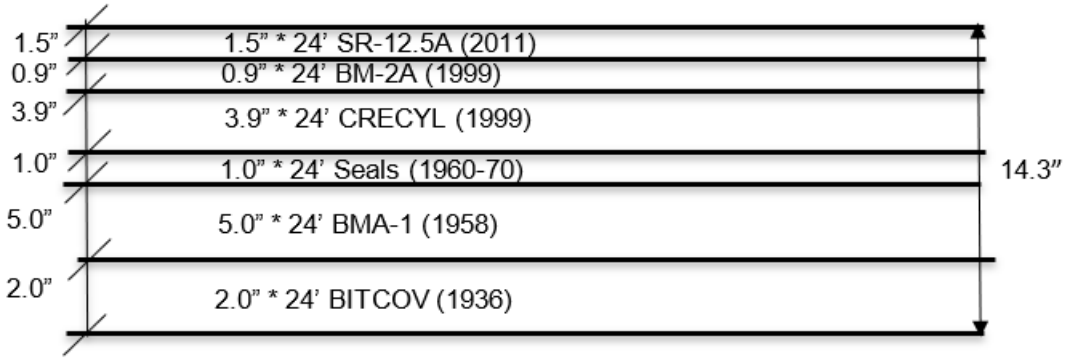

Figure A.5: Historical Record of Pavement Layers in Clay County, Segment Two

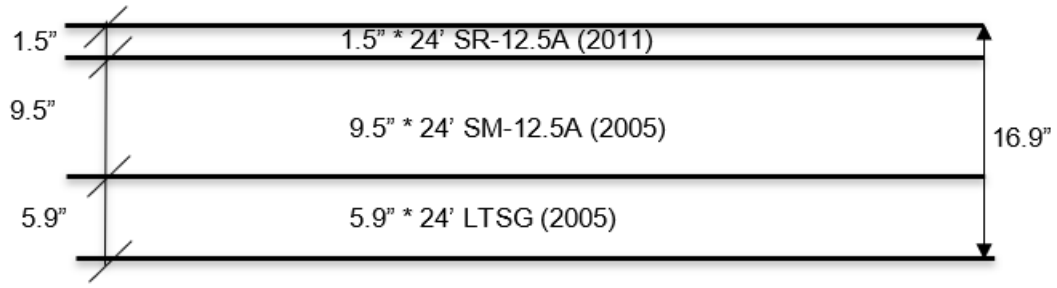

Figure A.6: Historical Record of Pavement Layers in Clay County, Segment Three

The fourth pavement segment in Clay County extends from 3.896 miles east of RS 1408, east to WCL of Clay Center. Its current total thickness is 14.3 inches, and its length is 1.111 miles. The corresponding cross section is depicted in Figure A.7.

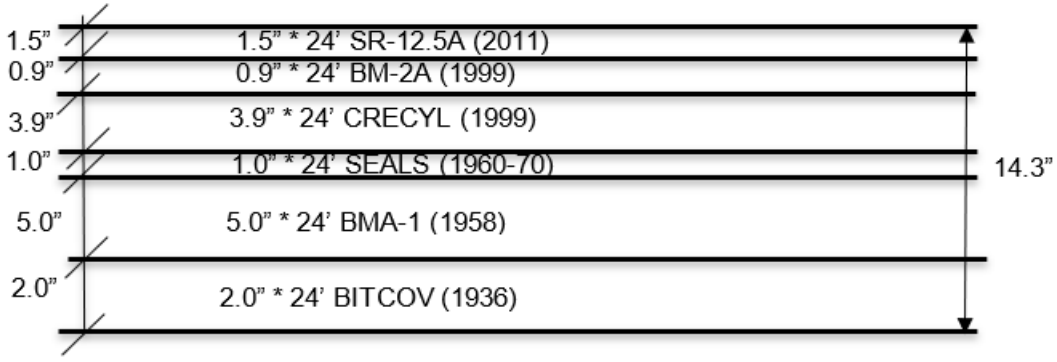

Figure A.7: Historical Record of Pavement Layers in Clay County, Segment Four

The cross section for segments two, three and four is depicted in Figure A.8.

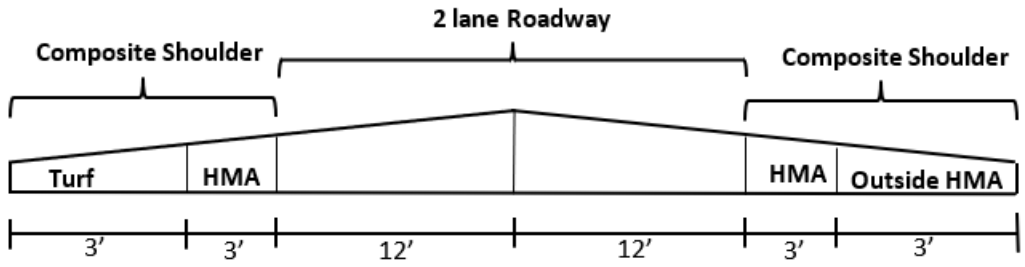

Figure A.8: Cross Section of Pavement in Clay County, Segments Two, Three and Four

The KDOT project number for pavement is Douglas County is KA-3634-03. The first segment extends from the beginning of the project, south and east to US-40/US-59. The current total thickness of this segment is 19.1 inches. The corresponding cross section is shown in Figure A.9.

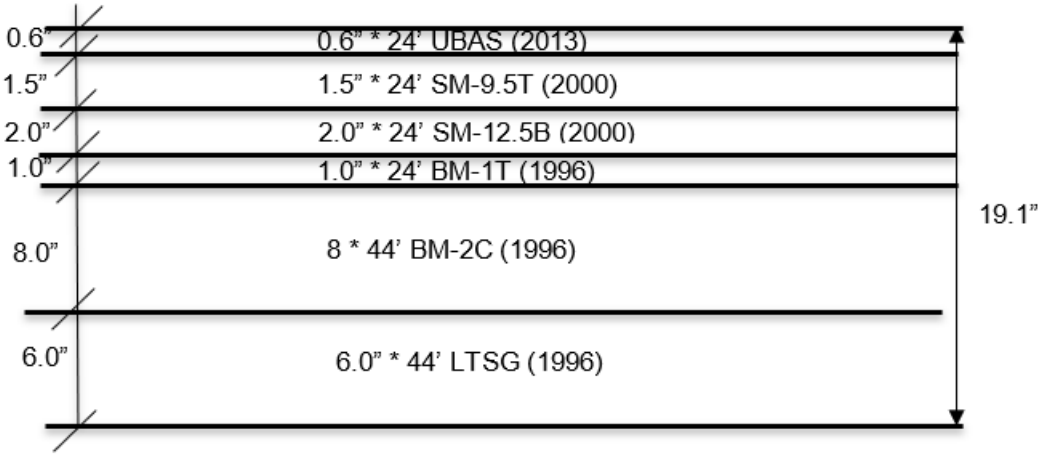

Figure A.9: Historical Record of Pavement Layers in Douglas County, Segment One

The cross section of the first and third pavement segments in Douglas County is shown in Figure A.10.

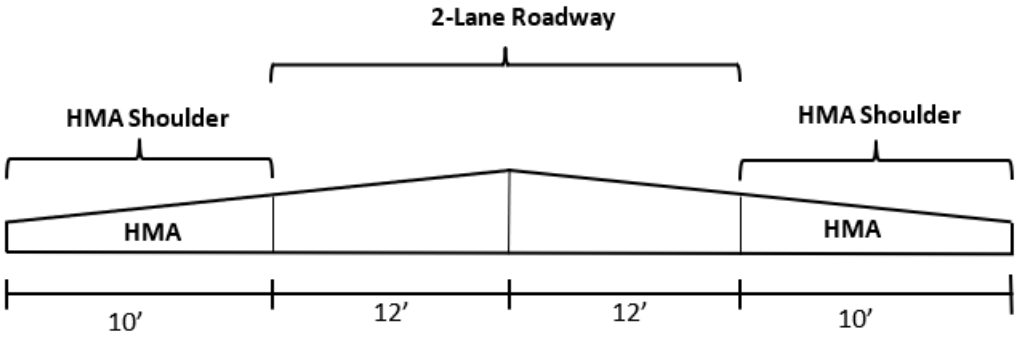

Figure A.10: Cross Section of Pavement in Douglas County, Segments One and Three

The second segment in Douglas County extends from US-40/US-59 (Iowa St.) east to K-10. Pavement throughout this segment is Dowel Joined Portland Cement Concrete Pavement (PCCPDJ). Consequently, it was excluded from analyses and its cross section is not included.

The third segment in Douglas County is US-40/US-59 that extends north and south of K-10. Currently the total pavement thickness in this segment is 16 inches. The historical record of pavement layers is depicted in Figure A.11.

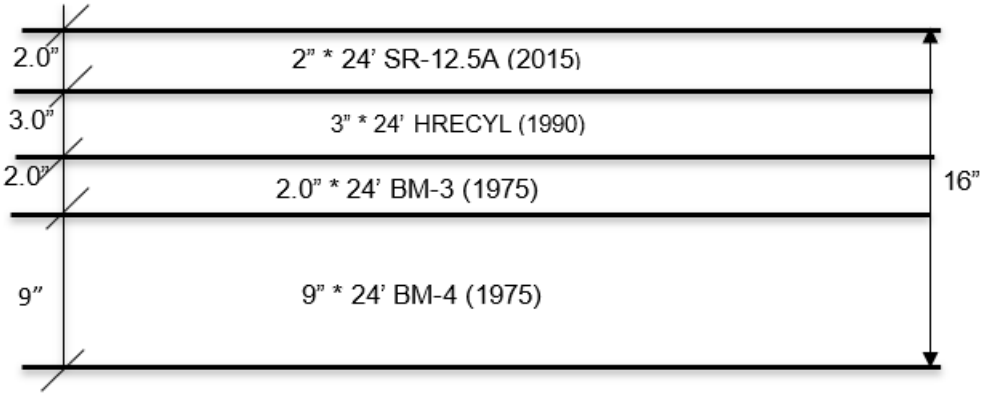

Figure A.11: Historical Record of Pavement Layers in Douglas County, Segment Three

The KDOT project number for Ford County is 50-29 KA-3234-02. There is only one pavement segment in Ford County. It extends from 0.2 miles east of east junction US-50/US-283, northeast to one mile east of RS-257. The total current thickness of the pavement is 21.5 inches. The historical record of pavement layers is shown in Figure A.12 while the corresponding pavement cross section is depicted in Figure A.13. Total length of this segment is 10.508 miles.

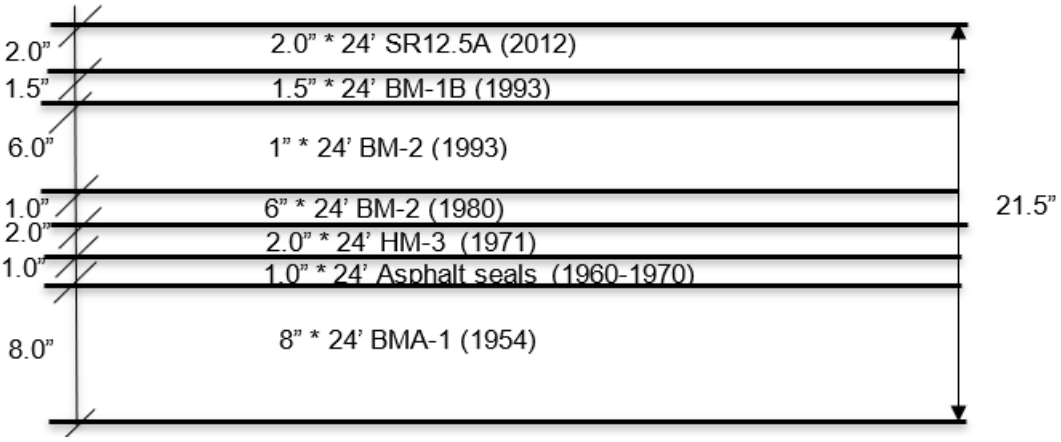

Figure A.12: Historical Record of Pavement Layers in Ford County

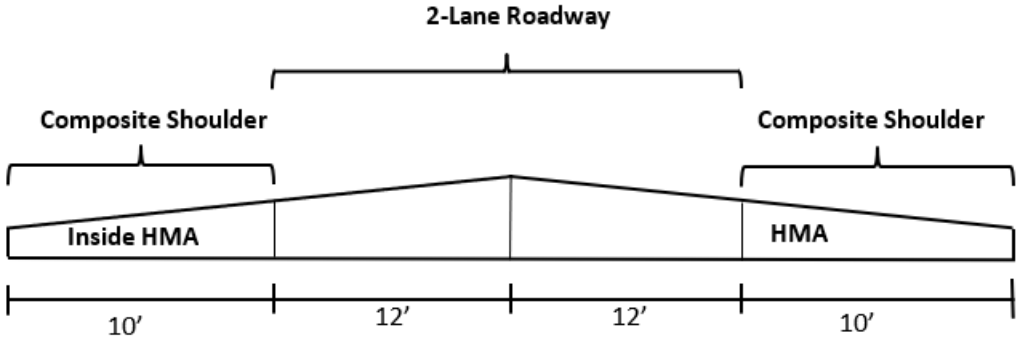

Figure A.13: Cross Section of Pavement in Ford County

The KDOT project number for Gove County is 70-32 KA-0726-01/NHPP-0702(047). A historical record of pavement layers depicted in Figure A.14. The corresponding pavement cross section is not available.

The KDOT project number for Harper County is 160-39 KA-2098-01. Two pavement segments were selected in Harper County. The first segment is part of US-160 on bridges (007), (008) and (011). The current total thickness of this segment is 13.125 inches. The second segment is also part of US-160 on bridges (012), (013) and (014). The current total thickness of this segment is 9.625 inches. The historical records of pavement layers in the first and second segments are shown in Figures A.15 and A.16, respectively.

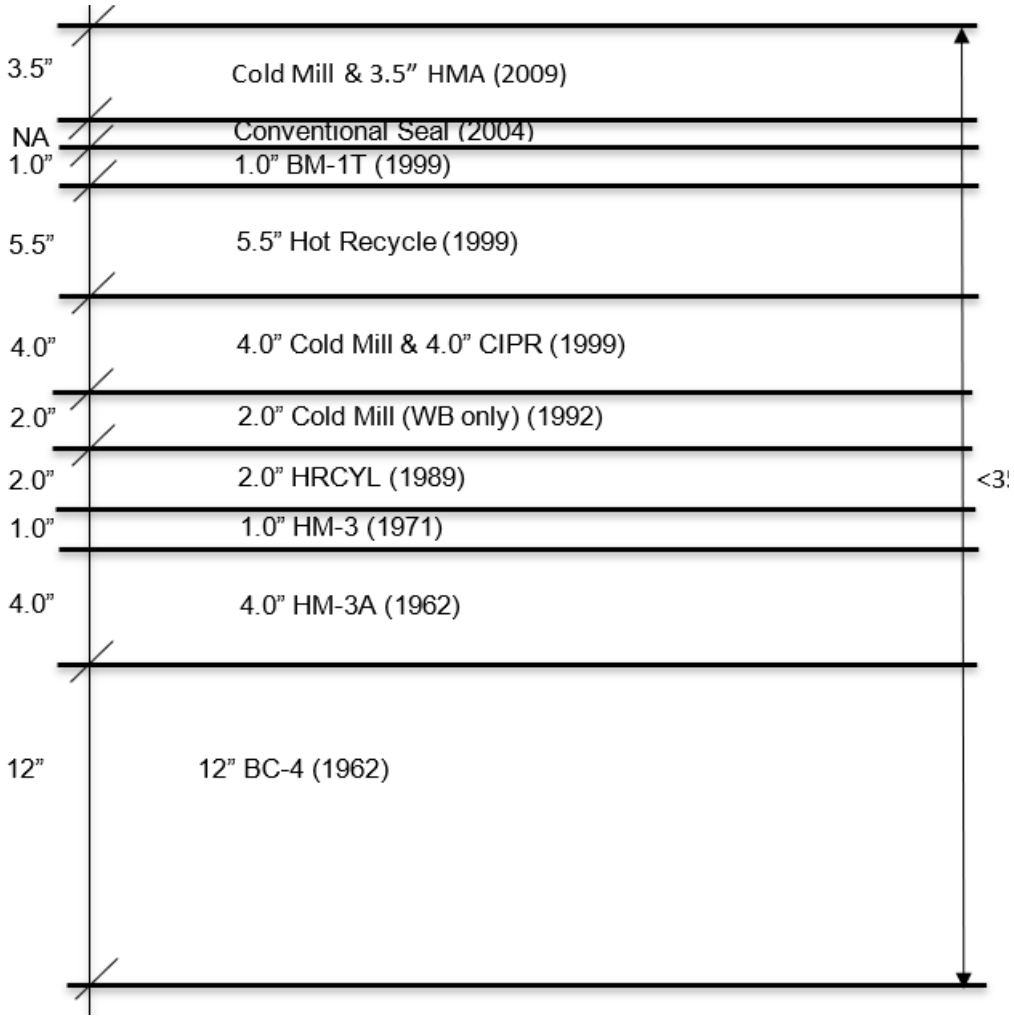

Figure A.14: Historical Record of Pavement Layers in Gove County

The cross sections of pavements in the first and second segments in Harper County are shown in Figure A.17.

The KDOT project number for Johnson County is 435-46 KA-4275-02. The first and second segments have Portland Cement Concrete Pavement (PCCP). Hence, they are excluded from the analyses in this study. The third segment has asphalt concrete pavement. The historical record of pavement layers is not available. Nevertheless, names of all layers present and order of their appearance are shown in Table B.1 in Appendix B.

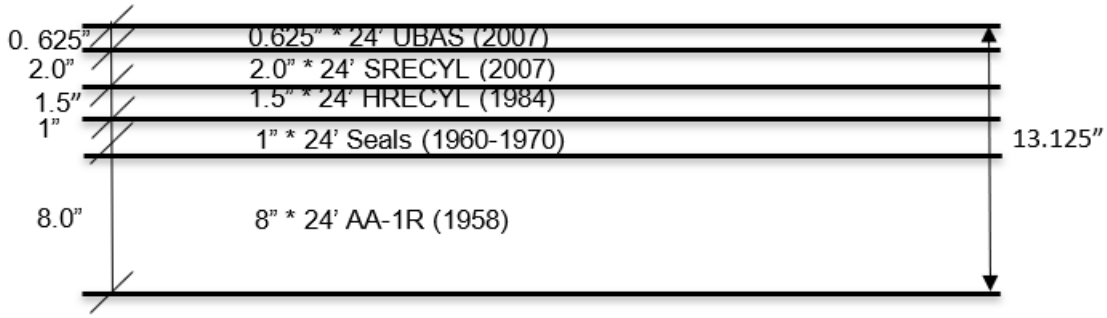

Figure A.15: Historical Record of Pavement Layers in Harper County, Segment One

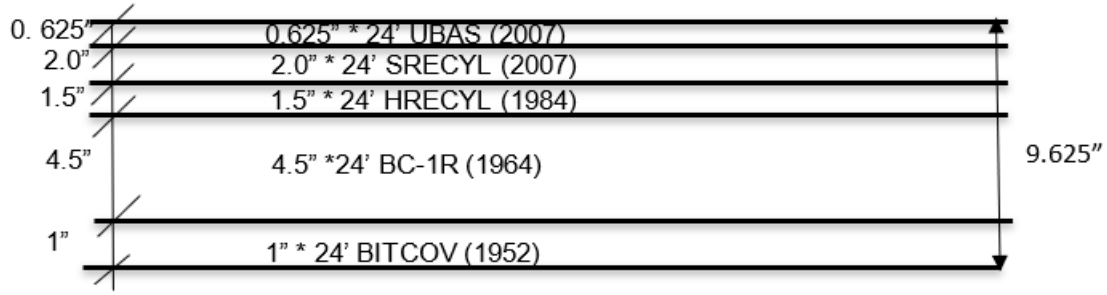

Figure A.16: Historical Record of Pavement Layers in Harper County, Segment Two

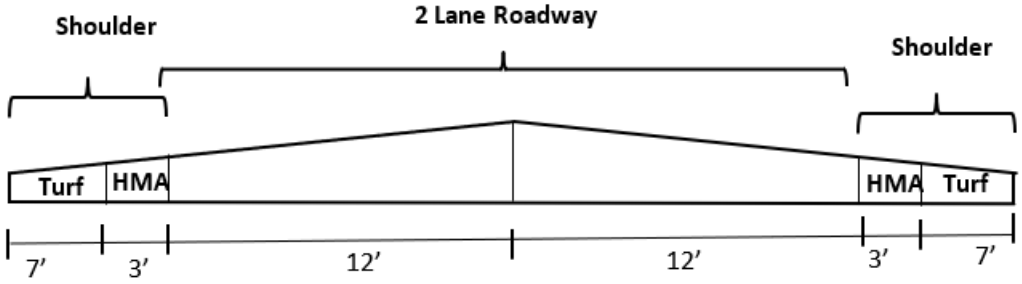

Figure A.17: Cross Section of Pavement in Harper County, Segments One and Two

The KDOT project number for Reno County is 14-78 KA-4686-01. The first segment extends from 3.9 miles east of Nickerson, west to ECL of Nickerson. Its total thickness is 16.5 inches, and its total length is 3.917 miles. A historical record of the corresponding pavement layers is shown in Figure A.18.

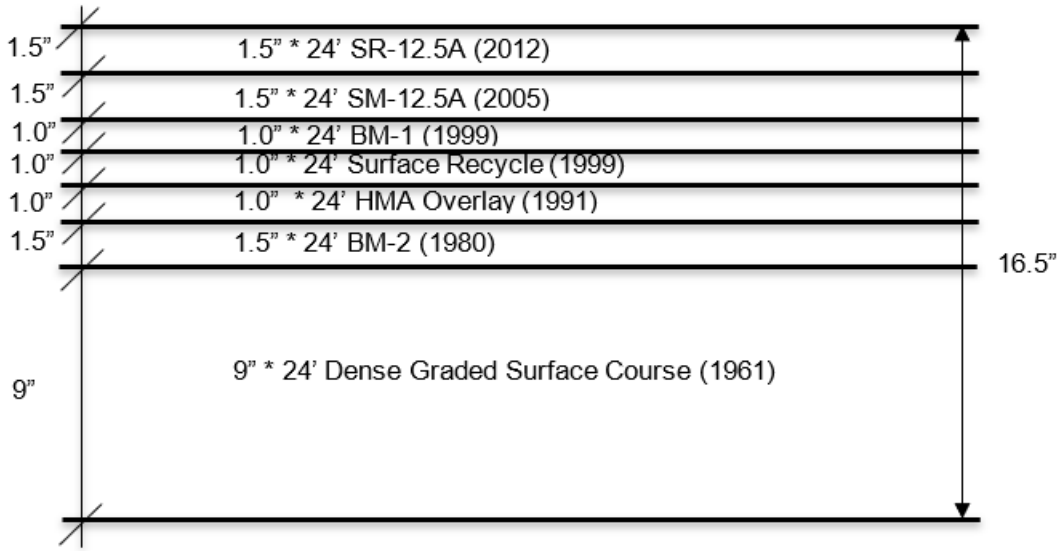

Figure A.18: Historical Record of Pavement Layers in Reno County, Segment One

The second segment in Reno County extends from ECL of Nickerson west to RS-673. The total thickness of the pavement in this segment is 16.5 inches and its length is 0.027 miles. The corresponding historical record of layers is shown in Figure A.19. Pavement cross section for the first and second segment in Reno County is shown in Figure A.20.

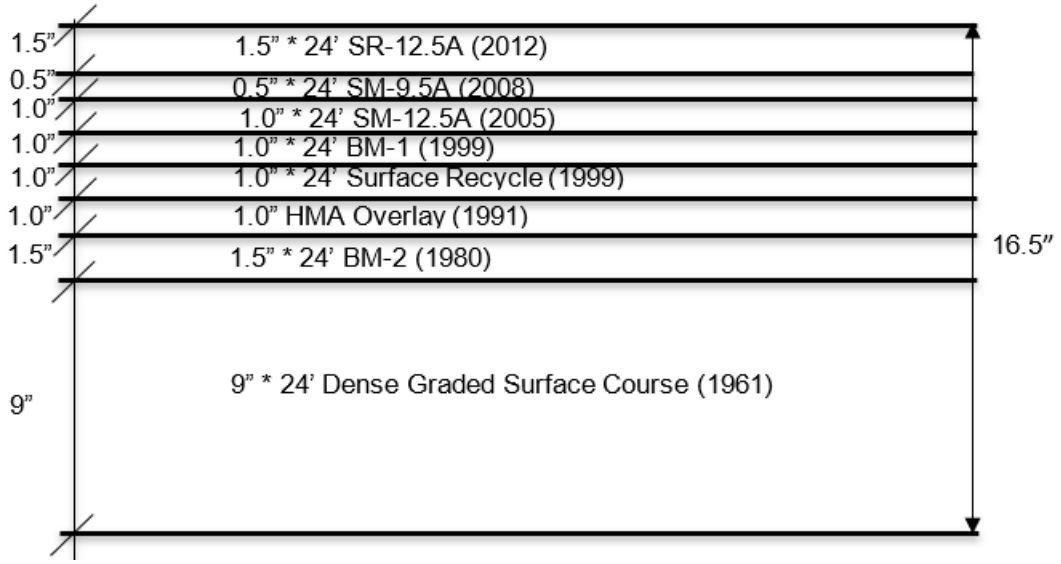

Figure A.19: Historical Record of Pavement Layers in Reno County, Segment Two

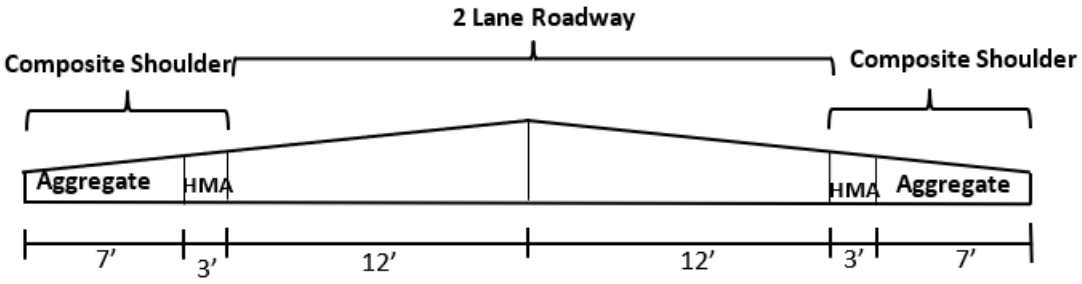

Figure A.20: Cross Section of Pavement in Reno County, Segments One and Two

The third segment in Reno County extends from RS-673 west to Curb and Gutter. The current total pavement thickenss in this segment is 14.5 inches and its total length is 0.091 miles. The historical record of pavement layers in the third segment of Reno County is shown in Figure A.21.

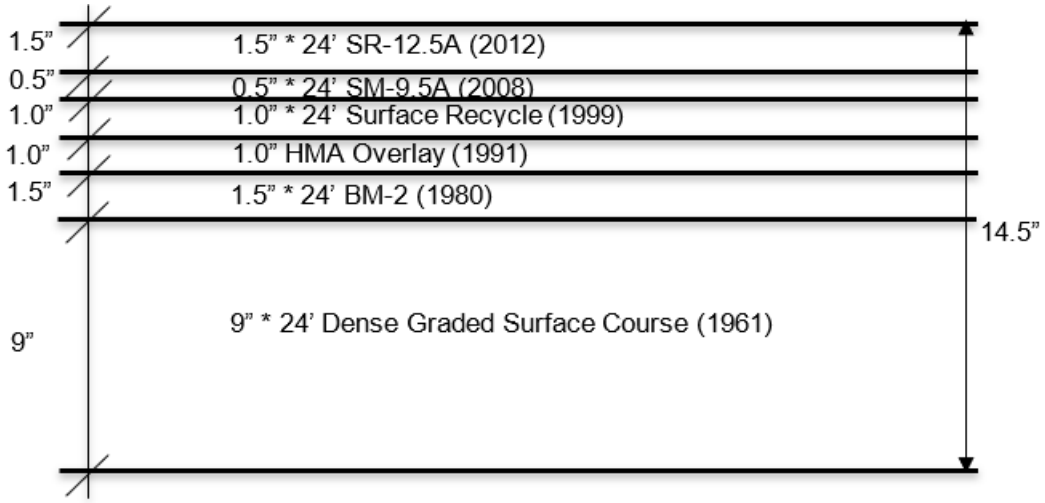

Figure A.21: Historical Record of Pavement Layers in Reno County, Segment Three

The cross section of the pavement in the third segment of Reno County is shown in Figure A.22.

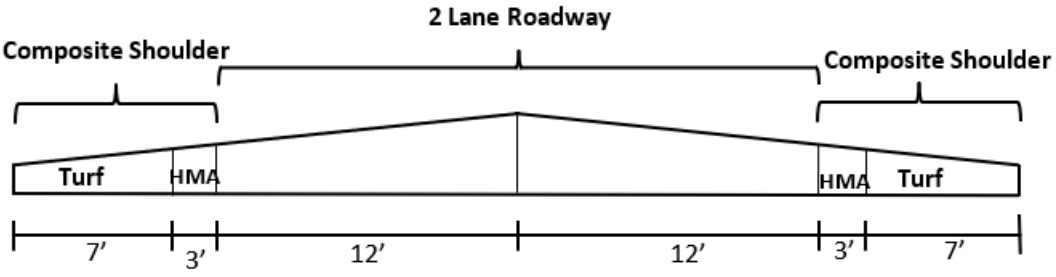

Figure A.22: Cross Section of Pavement in Reno County, Segment Three

The KDOT project number for Shawnee County is 24-89 KA-3235-01. Two separate segments were selected in Shawnee County. In Table 3.1, they are named Shawnee1 and Shawnee2. There are two different segments within Shawnee1. The first segment extends from ECL of Silver Lake 2.7 miles east. The current total thickness of this segment is 11.3 inches and its length is 0.32 miles. Historical record of pavement layers in the first segment of Shawnee1 is depicted in Figure A.23.

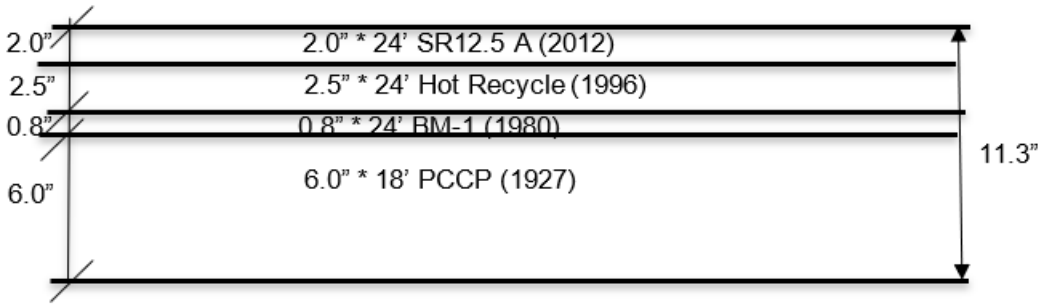

Figure A.23: Historical Record of Pavement Layers in Shawnee1, Segment One

The second segment in Shawnee1 extends from 2.7 miles ECL of Silver Lake east to RS-1254. The total current thickness of this segment is 14.3 inches and its length is 0.32 miles. The corresponding historical record of pavement layers in this segment is shown in Figure A.24.

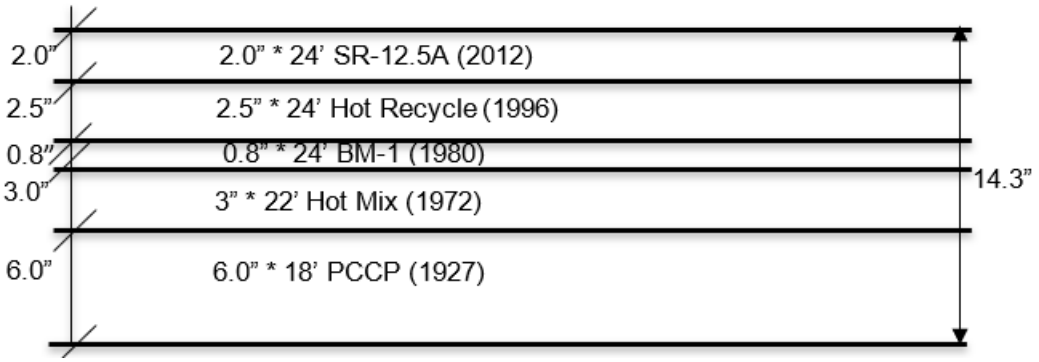

Figure A.24: Historical Record of Pavement Layers in Shawnee1, Segment Two

The segment in Shawnee2 extends from RS-1254 east to Countryside Road. The total thickness of this segment is 19.5 inches and its length is 1.48 miles. A historical record of pavement layers in Shawnee2 is depicted in Figure A.25.

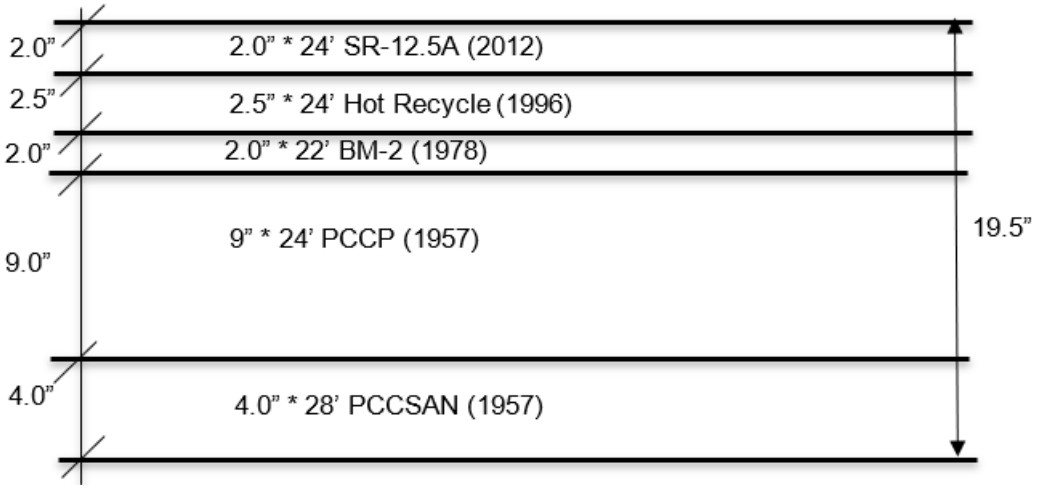

Figure A.25: Historical Record of Pavement Layers in Shawnee2

Pavement cross section for all segments in Shawnee1 and Shawnee2 is shown in Figure A.26.

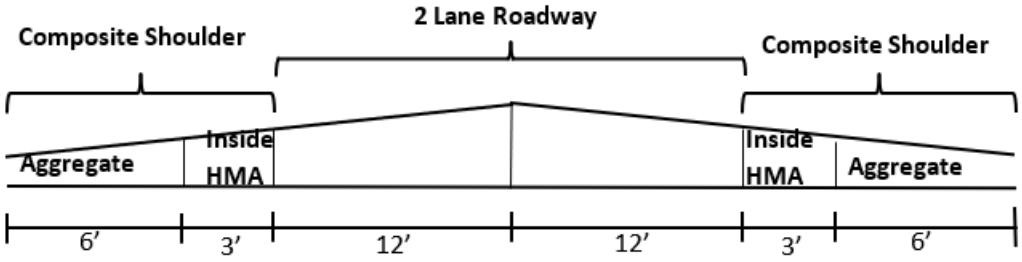

Figure A.26: Cross Section of Pavement in Shawnee1 and Shawnee2

The KDOT project number for Thomas County is 70-97 KA-0721-01. The first segment extends from 0.4 miles west of K-25 (Colby) east to I-70/K-25 junction. Its current total thickness is 23.6 inches and its length is 0.4 miles. The corresponding historical record is depicted in Figures A.27.

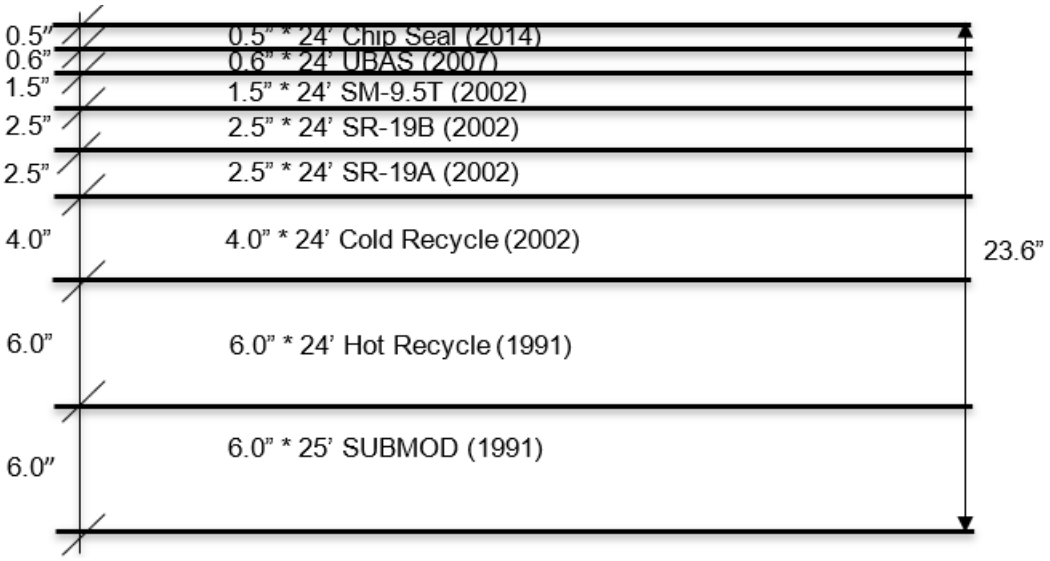

Figure A.27: Historical Record of Pavement Layers in Thomas County, Segment One

The second segment in Thomas County extends from I-70/K-25 junction east to 0.2 miles east of ECL of Colby. Its current total thickness is 24.2 inches and its length is 0.36 miles. The corresponding historical record of the pavement layers is shown in Figure A.28.

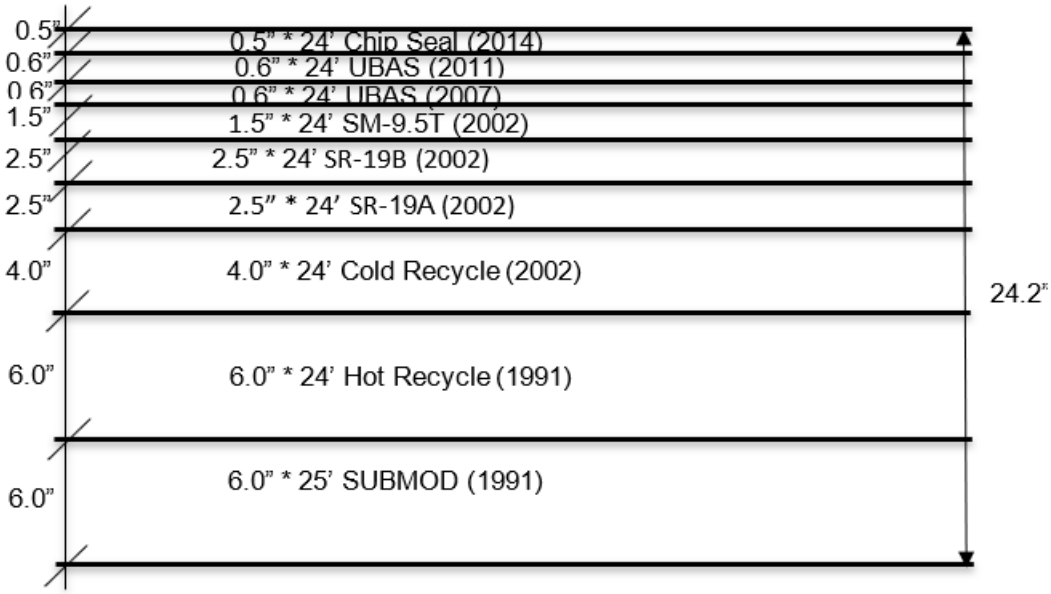

Figure A.28: Historical Record of Pavement Layers in Thomas County, Segment Two

The third segment in Thomas County extends from ECL of Colby southeast to RS-886. Its current total thickness is 23.6 inches and its length is 8.57 miles. The corresponding historical record of pavement layers for westbound lanes is depicted in Figure A.29. A historical record of pavement layers in the eastbound lanes of the third segment in Thomas County is shown in Figure A.30. The corresponding total current total thickness of the pavement is 25.1 inches.

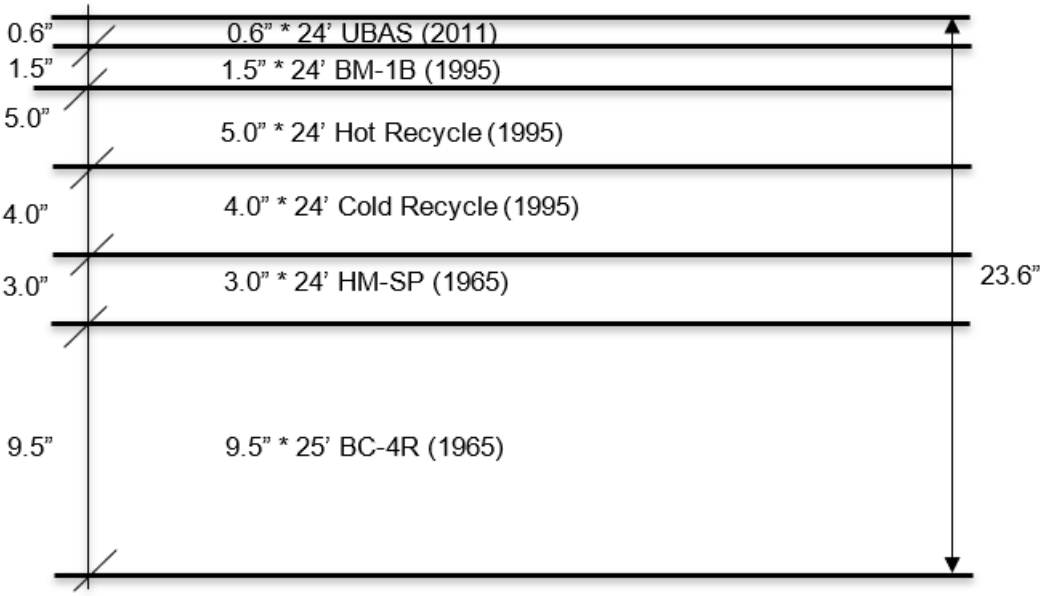

Figure A.29: Historical Record of Pavement Layers in Thomas County, Segment Three, WB Lanes

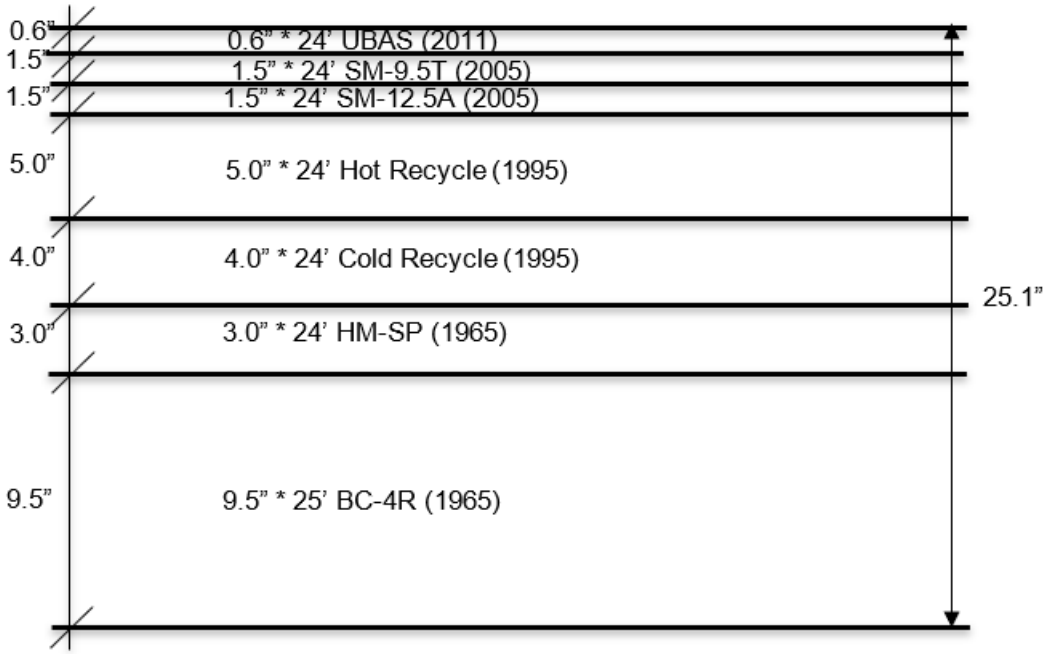

Figure A.30: Historical Record of Pavement Layers in Thomas County, Segment Three, EB Lanes

The current total thickness of the fourth segment in Thomas County is 24.1 inches. A corresponding historical record of pavement layers is shown in Figure A.31.

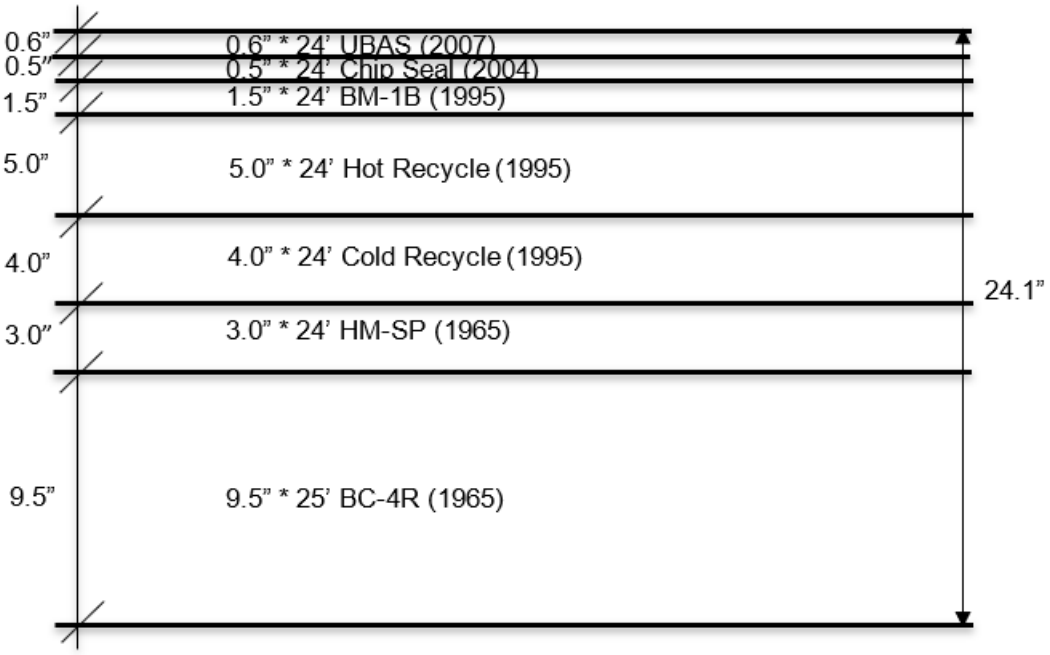

Figure A.31: Historical Record of Pavement Layers in Thomas County, Segment Four

The cross section of the pavement in all segments of Thomas County is shown in Figure A.32.

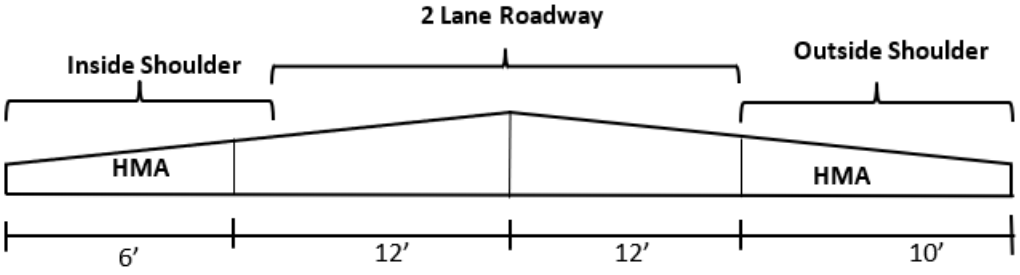

Figure A.32: Cross Section of Pavement in Thomas County

Appendix B: Tabular Presentation of Pavement Layers

Current pavement layers along with explanations of abbreviations, which were used to denote pavement layers in Figures in Appendix A, are presented in Table B.1.

Table B.1: Tabular Presentation of Pavement Layers

County	Segment	Layer
Cherokee	1st	**SR-4.75 A**: Superpave recycle mix, nominal aggregate size 4.75, above maximum density.
		Chip Seal
		SM-9.5T: Superpave mix, nominal aggregate size 9.5, friction course mix.
		Surface Recycle: surface recycled pavement
		BM-2D: bit. mix w/combined aggregates. 50% crushed material
		Hot Recycle: hot recycled pavement
		HM-4: sheet asphalt (45) surface, chat (51) crushed (55) chat (60) (66), E = 25,000psi
		Asphalt seals
		AB: aggregate binder, E =6,000 psi.
Clay	1st	**SR-12.5A:** Superpave mix, nominal aggregate size 12.5, above maximum density.
		BM-2A: bit**.** mix w/combined aggregates. 50% crushed material, 15% natural sand. Generally, for thin overlays.
		CRECYL: cold recycle pavement
		BC-1: bituminous construction, grading 1, E = 15,000 psi
		LTSG: lime treated subgrade
	2nd	**SR-12.5A:** Superpave mix, nominal aggregate size 12.5, above maximum density.
		BM-2A: bit**.** mix w/combined aggregates. 50% crushed material, 15% natural sand. Generally, for thin overlays.
		CRECYL: cold recycle pavement
		Seals
		BMA-1: bituminous material, fine grading, E = 15,000 psi
		BITCOV: bituminous cover, old wearing course
	3rd	**SR-12.5 A**: Superpave recycle mix, nominal aggregate size 12.5
		SM-12.5 A: Superpave mix, nominal aggregate size 12.5
		LSTG: lime treated subgrade
	4th	**SR-12.5A:** Superpave mix, nominal aggregate size 12.5, above maximum density.

County	Segment	Layer
		BM-2A: bit. mix w/combined aggregates. 50% crushed material, 15% natural sand. Generally, for thin overlays.
		CRECYL: cold recycle pavement
		SEALS
		BMA-1: bituminous material, fine grading, E = 15,000 psi
		BITCOV: bituminous cover, old wearing course
Douglas	**1st**	**UBAS:** ultra-thin bonded asphalt surface
		SM-9.5T: Superpave mix, nominal aggregate size 9.5, friction course mix.
		SM-12.5B: Superpave mix, nominal aggregate size 12.5, below maximum density.
		BM – 1T: bituminous mix with combined aggregates, base c. mix
		BM – 2C: bituminous mix with combined aggregates, base c. mix
		LTSG: lime treated subgrade
	3rd	**SR-12.5A:** Superpave mix, nominal aggregate size 12.5, above maximum density.
		HRCYL: hot recycle pavement
		BM -3: bituminous mix, chat (72). E= 20,000 psi.
		BM -4: bit. mix, at least 15% sand. E=15,000 psi.
Ford	**1st**	**SR-12.5A:** Superpave mix, nominal aggregate size 12.5, above maximum density.
		BM-1B: bit. mix w/combined aggregates. 50% crushed material, 15% natural sand. Rut resistant surface course mix.
		BM-2: bit. mix w/combined aggregates
		BM-2: bit. mix w/combined aggregates
		HM-3: leveling, chat (45) mixed (55) surface, crushed stone (51), mixed (60) (66). E= 25,000 psi.
		Asphalt seals
		BMA-1: bituminous mat grading 1, fine. E= 15,000 psi
Gove	**1st**	**Cold Mill & 3.5" HMA**
		Conventional Seal
		BM-1T: bit. mix w/combined aggregates. 40% crushed aggregate, 35% crushed limestone, 10% natural sand. Surface friction course under high traffic volume conditions.
		Hot Recycle
		Cold Mill & 4.0" CIP
		Cold Mill (WB only)
		HRCYL: hot recycled pavement
		HM-3: leveling, chat (45) mixed (55) surface, E = 25,000 psi
		HM-3A: mixed (57) (60) at least 50% crushed stone, E= 25,000 psi

County	Segment	Layer
		BC-4: bituminous construction grading 4, E 10,000 psi
Harper	**1st**	**UBAS:** ultra-thin bonded asphalt surface
		SRECYL: surface recycled pavement
		HRECYL: hot recycled pavement
		Seals
		AA-1R: aggregate asphalt grading 1 revised, finer, E 10,000
	2nd	**UBAS:** ultra-thin bonded asphalt surface
		SRECYL: surface recycled pavement
		HRECYL: hot recycled pavement
		BC-1R: bituminous construction grading 1 revised, E=15,000 psi
		BITCOCV: bituminous cover, old wearing course
Johnson Segment-3	**1st & 2nd**	**UBAS:** ultra-thin bonded asphalt surface
		SM-9.5T: Superpave mix, nominal aggregate size 9.5, friction course mix.
		SM-12.5A: Superpave recycle mix, nominal aggregate size 12.5, above maximum density.
		RCI: reflective crack interlayer
		PCCPAV: Portland cement concrete pavement
		CTB: cement treated base
		LTSG: lime treated subgrade
Reno	**1st**	**SR-12.5A:** Superpave mix, nominal aggregate size 12.5, above maximum density.
		SM-12.5A: Superpave mix, nominal aggregate size 12.5, above maximum density
		BM-1: bituminous mix w/combined aggregates. 30% crushed material, 15% natural sand.
		Surface Recycle
		HMA Overlay
		BM-2: bit. mix, mixed aggregate, 50%crushed material, 15% sand (72). E = 20,000 psi.
		Dense graded Surface course
	2nd	**SR-12.5A:** Superpave mix, nominal aggregate size 12.5, above maximum density.
		SM-9.5A: Superpave mix, nominal aggregate size 9.5, above maximum density
		SM-12.5A: Superpave mix, nominal aggregate size 12.5, above maximum density
		BM-1: bituminous mix w/combined aggregates. 30% crushed material, 15% natural sand.
		Surface Recycle:
		HMA Overlay

County	Segment	Layer
		BM-2: bit. mix, mixed aggregate, 50%crushed material, 15% sand (72). E = 20,000 psi.
		Dense graded Surface course
	3rd	**SR-12.5A:** Superpave mix, nominal aggregate size 12.5, above maximum density.
		SM-9.5A: Superpave mix, nominal aggregate size 9.5, above maximum density
		Surface Recycle
		HMA Overlay: hot mixed aggregate
		bM-2: bit. mix, mixed aggregate, 50%crushed material, 15% sand (72). E = 20,000 psi.
		Dense graded Surface course
Shawnee	1st	**SR-12.5A:** Superpave mix, nominal aggregate size 12.5, above maximum density.
		Hot Recycle
		BM-1: bituminous material, fine grading, E = 15,000 psi
		PCCP: Portland cement concrete pavement
	2nd	**SR-12.5A:** Superpave mix, nominal aggregate size 12.5, above maximum density.
		Hot Recycle
		BM-1: bituminous material, fine grading, E = 15,000 psi
		Hot Mix
		PCCP: Portland cement concrete pavement
	3rd	**SR-12.5A:** Superpave mix, nominal aggregate size 12.5, above maximum density.
		Hot Recycle
		BM-2: bit. mix, mixed aggregate, 50%crushed material, 15% sand (72). E= 20,000 psi.
		PCCP: Portland cement concrete pavement
		PCCSAN: Sand
Thomas	1st	**Chip Seal**
		UBAS: ultra-thin bonded asphalt surface
		SM-9.5T: Superpave mix, nominal aggregate size 9.5, friction course mix.
		SR-19B: Superpave mix, nominal aggregate size 19.0, below maximum density.
		SR-19A: Superpave mix, nominal aggregate size 19.0, above maximum density.
		Cold Recycle
		Hot Recycle
		SUBMOD: subgrade modification
	2nd	**Chip Seal**
		UBAS: ultra-thin bonded asphalt surface

County	Segment	Layer
		UBAS: ultra-thin bonded asphalt surface
		SM-9.5T: Superpave mix, nominal aggregate size 9.5 friction course mix.
		SR-19B: Superpave mix, nominal aggregate size 19.0, below maximum density.
		SR-19A: Superpave mix, nominal aggregate size 19.0, above maximum density.
		Cold Recycle
		Hot Recycle
		SUBMOD: subgrade modification
	3rd	**UBAS:** ultra-thin bonded asphalt surface
		BM-1B: bit. mix w/combined aggregates. 50% crushed material, 15% natural sand. Rut resistant surface course mix**.**
		Hot Recycle
		Cold Recycle
		HM-SP: hot mix special designated, E = 25,000 psi
		BC-4R: bituminous construction grading 4, E = 10,000 psi
	4th	**UBAS:** ultra-thin bonded asphalt surface
		SM-9.5T: Superpave mix, nominal aggregate size 9.5, friction course mix.
		SM-12.5A: Superpave recycle mix, nominal aggregate size 12.5, above maximum density.
		Hot Recycle
		Cold Recycle
		HM-SP: hot mix special designated, E = 25,000 psi
		BC-4R: bituminous construction grading 4, E = 10,000 psi
	5th	**UBAS:** ultra-thin bonded asphalt surface
		Chip Seal
		BM-1B: bit. mix w/combined aggregates. 50% crushed material, 15% natural sand. Rut resistant surface course mix**.**
		Hot Recycle
		Cold Recycle
		HM-SP: hot mix special designated, E = 25,000 psi
		BC-4R: bituminous construction grading 4, E = 10,000 psi

K-TRAN

KANSAS TRANSPORTATION RESEARCH AND NEW-DEVELOPMENT PROGRAM

AD ASTRA PER ASPERA

Kansas

Department of Transportation